MOLLUSCAN RESEARCH
https://doi.org/10.1080/13235818.2019.1634307

Taylor & Francis
Taylor & Francis Group

The fine structure of gametogenesis and somatic cells in the ovotestis of the terrestrial pulmonate slug, *Laevicaulis alte* (Férussac, 1822)

Soumen Roy, Samir Kumar Saha and Narayan Ghorai

Department of Zoology, West Bengal State University, Kolkata, India

ABSTRACT

The development of gametes and somatic cells in the ovotestis of *Laevicaulis alte* of different body weights is studied using transmission electron microscopy. Spermatogenesis is a proliferative phase in the ovotestis of smaller slugs acting as males, while oogenesis predominantly occurs in larger slugs acting as females. Male gametes are distributed throughout the acini in smaller slugs and residual cytoplasmic materials of developing spermatids bud off into the Sertoli cells. In larger slugs, each acinus comprises only one vitellogenic oocyte, completely surrounded by a follicle cell layer with a follicular cleft which is linked to the development of the oocyte. Oocytes utilise auto- and heterosynthetic mechanisms of yolk formation. Autosynthesis is accomplished by various ooplasmic organelles while heterosynthesis is promoted by an endocytic activity of the oolemma. The development of gonadal somatic cells is directly related to the growth of stage-specific gametogenesis. Sertoli cells are divided for the first time into two categories, cortical Sertoli cells or luminal Sertoli cells. Sertoli cells possess numerous tunnelling nanotubes which assist the transportation of cellular components to distant developing gametes. The suggestion that oocyte numbers in each acinus depend more on the corresponding habitats of the pulmonate species than on their taxonomic relatedness is discussed.

ARTICLE HISTORY
Received 24 July 2018
Final version received 3 June 2019

KEYWORDS
Follicular layer; hermaphrodite; interacinar cell; periacinar cell layer; tunnelling nanotubes; types of Sertoli cell; ultrastructure; yolk formation

Introduction

The pulmonate molluscs are simultaneous hermaphrodites and their gonad is termed an ovotestis (Tompa 1984; Heller 1990, 2001). The ovotestis comprises numerous small acini which are the source of both male and female gametes (Luchtel 1972a, b; Jong-Brink *et al*. 1976; Rakshit *et al*. 2005; Roy *et al*. 2016, 2018). *Laevicaulis alte* (Férussac, 1822) is a common terrestrial systellommatophoran slug that has been relatively little studied with regard to the structural details of the ovotestis (Raut and Panigrahi 1990; Bhavare and Magare 2017). Reproductively, *L. alte* has some similarities with the terrestrial stylommatophoran pulmonates (Jörger *et al*. 2010; Kocot *et al*. 2013). In the field, it is observed that *L. alte* preferentially copulates with a mating partner of different body size, as reported in other aquatic and terrestrial hermaphrodite pulmonates (Otsuka *et al*. 1980; Staib and Ribi 1995; Tomiyama 1995; De Witt 1996; Yusa 1996; Angeloni and Bradbury 1999; Jordaens *et al*. 2005; Kimura *et al*. 2015). The growth of individuals is commonly proportional to the body weight (or size) of the individual and directly correlated to organogenesis and the proliferation of gametogenesis in the gonad (Sabelli and Sabelli 1980; Ohbayashi-Hodoki *et al*. 2004; Nakadera *et al*. 2015; Roy *et al*. 2016, 2018). The weight of the albumen gland, expressed as the vitelline-somatic index (VSI) has been utilised as an important diagnostic marker in male-female role transition in hermaphroditic pulmonates and is directly correlated to the body weight of individuals–those with a small albumen gland are considered as male and those with a large albumen gland act as female (Cunha *et al*. 1998; Bing *et al*. 2008; Roy *et al*. 2018). It is reported that hermaphrodite pulmonates with smaller body size/weight possess a proliferative phase of spermatogenesis and act as male while oogenesis progresses in the larger individuals, which act as females (Tomiyama 1995; Nakadera *et al*. 2015; Roy *et al*. 2016, 2018). The proliferation of either spermatogenesis or oogenesis in the ovotestis is directly correlated to the gender role choice in copulation of hermaphrodite pulmonate molluscs (Sabelli and Sabelli 1980; Ohbayashi-Hodoki *et al*. 2004; Roy *et al*. 2016, 2018).

Yolk formation in the oocyte is an important process of pulmonate molluscs and accomplished by both auto- and heterosynthetic mechanisms (Bluemink1967; Nørrevang 1968; van der Wal 1974; Jong-Brink *et al*. 1976) but yolk formation in the oocyte of *L. alte* has not so far been described.

The ovotestis of *L. alte* is slightly embedded in the digestive gland (Quatrini and Lanza 1964, 1965; Kulkarni 1973) while it is represented as a completely separated globular mass in *Onchidium* (Bing *et al*. 2008;

CONTACT Soumen Roy soumenroyzoology@gmail.com, souroy1986@gmail.com Department of Zoology, West Bengal State University, Barasat, 24 Parganas (N), Berunanpukuria, Kolkata 700126, West Bengal, India

Published online 30 Jun 2019

Chen *et al*. 2015; Roy *et al*. 2018) as well as *Onchidella* (Selmi *et al*. 1988). The ovotestis of all these pulmonates consists of many ovoid acini. A typical interacinar zone is formed between acini and characterised by a tight interacinar junction or interacinar spaces (Roy *et al*. 2016, 2018). The entire acinar space is divided into two compartments which are described variously as the peripheral acinar zone and acinar lumen (e.g., Roy *et al*. 2016, 2018) or the cortical compartment and medullar compartment of an acinus (e.g., Luchtel 1972a, 1972b). The male and female gametes are sequentially developed in the acini and it is observed that the male gametes are commonly developed in the medullar compartment and female gametes in the cortical compartment of acini (Nagabhushanam and Kulkarni 1971; Luchtel 1972a, 1972b; Kulkarni 1973; Jong-Brink *et al*. 1976, 1977; Rigby 1982; Roy *et al*. 2016, 2018).

There is an inconclusive debate concerning the numbers of oocytes in each acinus of the ovotestis among pulmonate molluscs. Some workers have argued that the acinus contains more than one oocyte (Joosse and Reitz 1969; Jong-Brink *et al*. 1976; Deshpande and Nagabhushanam 1983; Pal and Hodgson 2002; Bing *et al*. 2008; Roy *et al*. 2018) and others argue that only one oocyte is present in each acinus (Parivar 1978; Griffond and Bolzoni-Sungur 1986; Boato and Rasotto 1987; Horn *et al*. 2005; Rakshit *et al*. 2005; Silva *et al*. 2009; Roy *et al*. 2016).

The ovotestis in pulmonate molluscs is usually comprised of four major somatic cell types: Sertoli cells, follicle cells, periacinar cells and interacinar cells. The Sertoli cells and follicle cells are present within the acini whereas the periacinar cells and interacinar cells are situated in the interacinar zone (Roy *et al*. 2016, 2018). The Sertoli cells are directly allied with spermatogenesis and provide mechanical as well as nutritive support in the development of male gametes (Kulkarni 1973; Jong-Brink *et al*. 1977; Parivar 1980; Rigby 1982; Buckland-Nicks and Chia 1986; Griffond and Bolzoni-Sungur 1986; Silva *et al*. 2009; Roy *et al*. 2016, 2018). Numerous tunnelling nanotubes (TNTs) of Sertoli cells support cellular communications with the developing male gametes remote from the cells (Roy *et al*. 2018). The follicle cells provide a barrier between male and female gametes (Jong-Brink *et al*. 1976; Rakshit *et al*. 2005; Roy *et al*. 2016, 2018) and act as a heterosynthetic source of yolk production for the oocyte (Jong-Brink *et al*. 1976; Eckelbarger and Blades-Eckelbarger 1989), transportation of oocytes (Barth and Jansen 1962; Starke 1971), and nutrition of oocytes (Taylor and Anderson 1969; Coggeshall 1972; Jong-Brink *et al*. 1976; Roy *et al*. 2018). The periacinar cells surround the acini and promote the release of spermatozoa into the acinar duct (Roy *et al*. 2016, 2018). The interacinar cells are found adjacent to the acini and help in the development of the spermatogenesis (Roy *et al*. 2016, 2018). There is a lack of consensus among workers as to whether the follicle cell layer surrounds the entire oocyte (Jong-Brink *et al*. 1976; Parivar 1978; Roy *et al*. 2016, 2018) or only the apical part (luminal surface) (Griffond and Bolzoni-Sungur 1986; Rakshit *et al*. 2005). The histomorphological study of ovotestis of *L. alte* by a light microscope was reported by Kulkarni (1973) but the fine structural features of gametes, as well as the various somatic cells in the ovotestis and their relation with gametogenesis, has not been studied.

The hypothesis of this study is that the development of gametogenesis, either spermatogenesis or oogenesis, is directly correlated with the body weight class of *L. alte*. The morphofunctional characteristics of various somatic cells in the ovotestis are directly allied with the proliferation of either spermatogenesis or oogenesis in the acini. The numbers of oocytes in each acinus of *L. alte* would be expected to be similar to those of other terrestrial pulmonate molluscs rather than to their aquatic relatives.

The aims of the present study are to investigate the fine structures of gametogenesis and various somatic cells in the ovotestis of *L. alte* of different body weight groups. The number of oocytes in each acinus of *L. alte* is determined here and compared to the numbers in other terrestrial or aquatic pulmonate molluscs. The work also investigates the morphometrics of different cellular parameters in the ovotestis of this land slug.

Materials and methods

Healthy, active *L. alte* were collected from fields around Kolkata, West Bengal, India (22.5726° N, 88.3639° E) during the rainy season (June-July). A group of 25 smaller *L. alte* (0.46 ± 0.01 g body weight) and 25 larger *L. alte* (1.06 ± 0.118 g body weight) specimens were collected. The specimens were acclimatised for three days in separate earthen pots and provided with leafy vegetables. Water was sprayed regularly to maintain humidity levels.

The relationship between body weight and albumen gland weight was expressed by the vitelline somatic index (VSI) (Bing *et al*. 2008; Roy *et al*. 2018):

$$\text{VSI (\%)} = \frac{\text{weight of albumen gland of an individual}}{\text{Body weight of the individual}} \times 100$$

The ovotestes were dissected from living individuals and instantly fixed in the fixative (pH 7.2), a mixture of 3% glutaraldehyde and 2% paraformaldehyde in 0.1M phosphate buffer. The ovotestes were cut into small pieces (1 mm^3 in size) and kept in fresh fixative for four hours at 4°C. After washing in buffer solution, the samples were post-fixed in 1% OsO_4 for one hour

at 4°C. After dehydration using increasing concentrations of acetone, the tissues were embedded in Araldite CY 212. The ovotestes were processed for semithin as well as other ultrastructural studies following standard methods (Roy *et al*. 2016). The semi-thin sections (1 µm) of the ovotestis from both the smaller and larger groups were studied using a light microscope (NIKON 50i) after staining with Toluidine blue (Dykstra 1993). The copper grids, each containing five to six ultrathin sections (60–70 nm) were examined using a transmission electron microscope (Tecnai) operated at 200 kV. Measurements of different cellular parameters in the ovotestis were made with 'ImageJ 1.51t' software (Wayne Rasband, NIH, USA) using electron micrographs and the dimensions of acini and female gamete were realised on light microscopic photographs.

Results

A relationship exists between body weight, albumen gland and VSI index of *L. alte*. The VSI was much lower in smaller slugs (0.18–0.51 g) and showed a sharp increase in slugs of body weight in the range 0.51–0.77 g. A gradual decrease in VSI was found in much larger slugs of 0.83 g or more body weight (Figure 1)

General description of ovotestis of L. alte

The ovotestis of *L. alte* was surrounded by a thin myoepithelial cell layer. The ovotestis consisted of numerous small, sac-like acini which had a thin germinal layer beneath the basement membrane of acinar boundary enclosing the acinar space. Each acinus was separated from all others by a distinct interacinar zone (Figure 2A). The thickness (1.21 ± 0.1 µm) of the acinar boundary of both smaller and larger groups of *L. alte* was almost the same. In the ovotestis, male gametes were distributed throughout the acinar space whereas female gametes were developed only in the cortical compartment of the acini. The structural characteristics of the ovotestis of *L. alte* were broadly similar in both smaller and larger groups, but there were some significant characteristic variations of the constituents of their acini. The fine structural characteristics of gametogenic and somatic cells in the ovotestes of smaller and larger *L. alte* are described in the following.

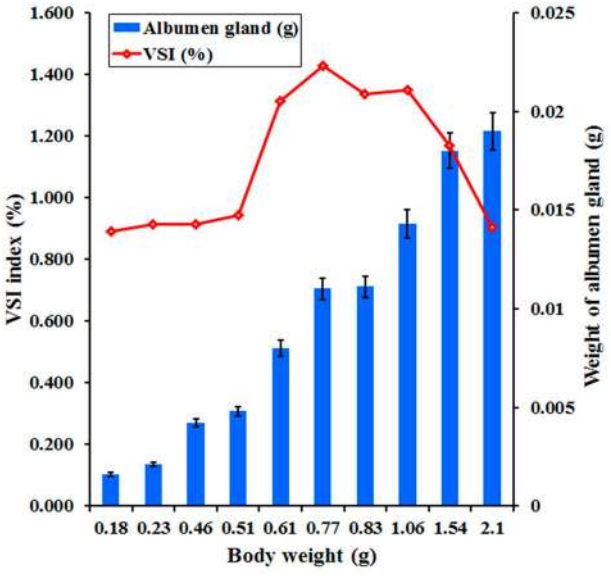

Figure 1. Histogram showing the relationship between body weight, albumen gland and vitelline somatic index (VSI) of *L. alte*. *N* = 3.

Ovotestis of smaller L. alte

The acini in the ovotestis were mostly occupied by developing male gametes and various related somatic cells (Figures 2A–D). The diameter of the acinus (6.51 ± 0.26 µm) of the smaller slugs was less than that of the larger slugs (7.71 ± 0.78 µm in diameter). The germinal layer (0.57 ± 0.27 µm in thickness) comprised slightly elongated epithelial cells with an elongated nucleus (0.74 ± 0.16 µm in diameter) (Figure 2D). The female gametes were very undeveloped and only found occasionally in some acini (Figure 2A).

Spermatogenesis

The acinus comprised different developmental stages of the spermatogenic cells (Figures 2A–B).

The spermatogonia (2.5 ± 0.27 µm in diameter) were mostly pear-shaped with an irregular cell surface, usually developed in the groove of Sertoli cells near the cortical area of acini (Figures 2B–D). The cytoplasm of the spermatogonia was granulated and composed of different organelles such as mitochondria (0.12 ± 0.02 µm in diameter), multiple stacks (0.13 ± 0.02 µm in width) of Golgi cisternae and many electron-dense bodies (Figure 2D). A prominent syncytial bridge between spermatogonia was observed (Figure 2C). The spermatogonia were comprised of a centrally placed, circular nucleus (0.56 ± 0.08 µm in diameter) with a small circular acentric nucleolus (0.16 ± 0.02 µm in diameter) (Figures 2C–D).

The spermatocytes (5.42 ± 0.99 µm in diameter) were circular or oval shaped and larger than spermatogonia (Figures 2B and 3). In some cases, the developing spermatocytes were surrounded by the tunnelling nanotubes (TNTs) of Sertoli cells (Figure 3). The cytoplasm of spermatocytes was comprised of numerous mitochondria (0.44 ± 0.06 µm in diameter), ribosomes, peroxisomes (0.31 ± 0.02 µm in diameter), electron-dense vesicles (0.23 ± 0.03 µm in diameter) of different sizes and multiple stacks (0.46 ± 0.13 µm in width) of Golgi cisternae with distinct secretory vesicles measuring 0.3 ± 0.02 µm in diameter (Figures 3 and

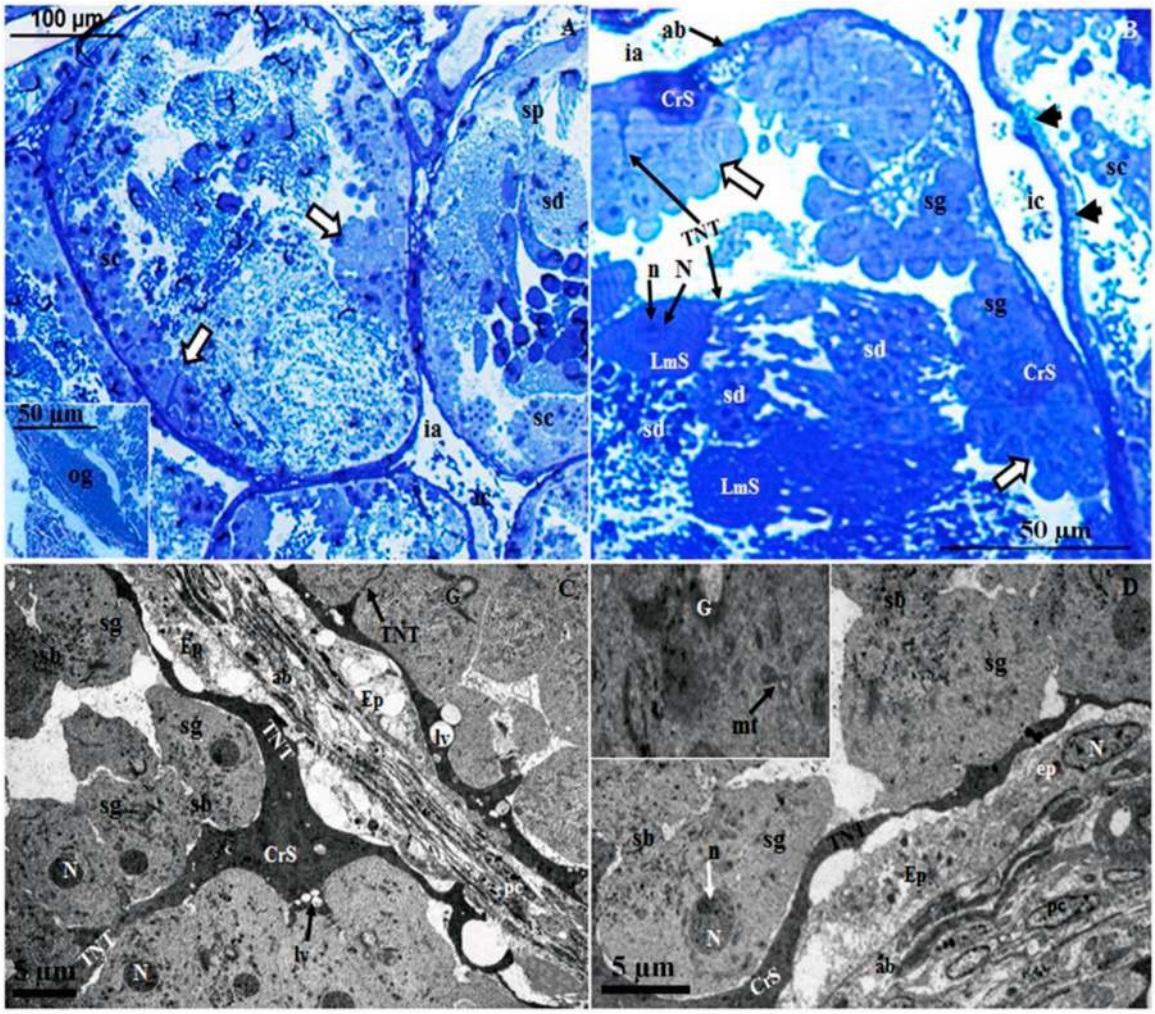

Figure 2. Ovotestis of smaller *L. alte* (0.46 ± 0.01 g). **A–B,** Semithin sections. A, Acinus is mostly occupied by spermatogenic cells of various developing stages. Inset: The oogonium (og) is located in a cortical area of an acinus. Aggregation of interacinar cells (ic) in interacinar space (ia). B, Enlarged view of a part of acinus viewing pyramidal growth (bold arrow) of spermatogonial cells on cortical Sertoli (CrS) cells. Arrow head indicates germinal epithelial layer. **C–D**, Transmission electron micrograph. C, Development of spermatogonial cells in the groove of CrS cells. D, Germinal epithelial cell layer beneath the acinar boundary. Inset: An enlarged view of the marked area of cytoplasm of spermatogonia shows numerous mitochondria and several stacks of Golgi complex. ab—acinar boundary; CrS—cortical Sertoli cell; ep—epithelial cell; Ep—germinal epithelial layer; G—Golgi complex; ia—interacinar space; ic—interacinar cells; LmS—luminal Sertoli cell; lv—electron-lucent vesicle; mt—mitochondria; n—nucleolus; N—nucleus; pc—periacinar cell; sb—syncytial bridge; sc—spermatocyte; sd—spermatid; sg—spermatogonium; sp—sperm; TNT—tunnelling nanotube.

4A). The Golgi cisternae were slightly curved and 1.5 ± 0.5 µm in length. The nucleus (3.32 ± 1.08 µm in diameter) of the spermatocytes was acentric, circular, lightly stained and larger in size than those of the spermatogonia (Figures 3 and 4A). The nuclear membrane at this stage was very indistinct. The nuclear materials were scattered throughout the nuclear space with a prominent nucleolus measuring 0.36 ± 0.16 µm in diameter (Figure 3).

The spermatids developed from large spherical cells to very elongated sperms. The progression of spermatid differentiation includes condensation, elongation and spiralisation of the nucleus, formation of the acrosomal process, reduction of cytoplasm from the cell body and formation of the axoneme (Figures 2A–B, 4B–E, 5A–C). The spermatids (3.65 ± 0.74 µm in diameter) were dispersed throughout the acinar lumen and developed as groups of cells (Figures 2A–B and 4B). The cytoplasm of spermatids consists of mitochondria (0.47 ± 0.04 µm in diameter), glycogen granules, electron-dense vesicles (0.29 ± 0.0.16 µm in diameter), wide rough endoplasmic reticulum (0.06 ± 0.03 µm in diameter), peroxisomes (0.51 ± 0.09 µm in diameter), stacks (0.58 ± 0.18 µm in width) of Golgi cisternae and secretory vesicles (0.40 ± 0.01 µm in diameter) (Figures 4B–C). The thickness of Golgi stacks in spermatids (0.58 ± 0.18 µm) was greater than those in spermatogonia (0.13 ± 0.02 µm) and spermatocytes (0.46 ± 0.13 µm) (Figures 2D and 4A, C). Each cisterna in the Golgi stack was approximately 3.9 ± 0.27 µm in length. The manchette forms of spermatids were prominent with noticeable modifications of the nucleus, axonemal microtubules and glycogen helix (Figure 4E). Each manchette form was 0.73 ± 0.06 µm in

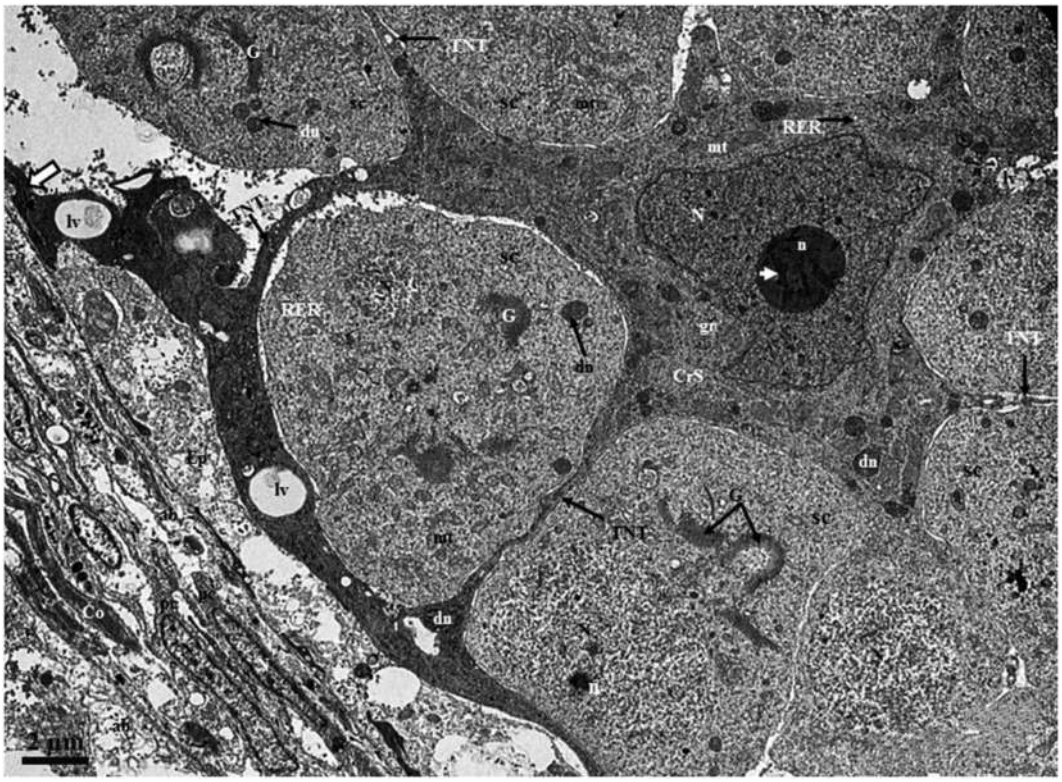

Figure 3. Transmission electron micrographs of ovotestis of smaller *L. alte* (0.46 ± 0.01 g). A typical CrS cell with prominent nucleus and nucleolus includes some electron-dense fibrous material (white arrowhead). The cell surface possesses well-developed TNTs which penetrate between adjacent spermatogenic cells. Cytoplasm of developing spermatocytes contains multiple stacks of Golgi complex (G) and numerous mitochondria (mt). Note the attachment (bold arrow) of the acinar boundary (ab) and CrS cell. ab—acinar boundary; Co—collagen fibres; dn—electron-dense vesicle; Ep—germinal epithelial layer; G—Golgi complex; gr—glycogen rosette; lv—electron-lucent vesicles; mt—mitochondria; n—nucleolus; N—Nucleus; pc—periacinar cell; RER—rough endoplasmic reticulum; sc—spermatocyte; TNT—tunnelling nanotube.

diameter and 2.75 ± 0.43 µm in length. The glycogen helix was 0.36 ± 0.07 µm in diameter. In early spermatids, the nucleus was positioned slightly to one side of the cell and the nucleolus did not appear at this stage (Figure 4B). The nuclear materials were simultaneously condensed near the apical part of the nucleus and the nuclear envelope was thickened to approximately 0.06 µm in diameter, and was without nuclear pores (Figure 4B). Several semithin and ultrathin sections revealed that growing spermatogenic cells were successively arranged according to their development from basal lamina to lumen of acini (Figures 2A–B and 4D). Syncytial bridges (2.04 ± 0.18 µm in diameter) between developing spermatogenic cells were prominent (Figures 2C and 4D). Some electron-lucent droplets (0.23 ± 0.02 µm in diameter), which were found near developing spermatids, may be secretions from Sertoli cells (Figure 4B).

The developing sperms were elongated with a cone-shaped, helical nucleus. The neck and middle part of the sperms had irregular lateral fins (Figures 5A–C). These fins were extended (0.78 ± 0.23 µm) laterally and were 0.29 ± 0.09 µm thick (Figure 5C). The heads of the developing sperms were usually sunken in Sertoli cells (Figure 5A). There was very little cytoplasm in the sperm. Some cytoplasmic materials were budded off as residual cytoplasmic materials from the sperm's head to the Sertoli cell (Figure 5A). The acrosomal process of developing sperms was shorter (0.49 ± 0.11 µm in length) with a prominent proximal notch, located on the apical nucleus or slightly lateral to the head of nucleus (Figure 5A). The glycogen helix of the sperm measured 0.82 ± 0.15 µm in diameter (Figure 5A). Numbers (4–6) of globular glycogen beads (0.10 ± 0.01 µm in diameter) were found in the glycogen helix at the middle body of the sperm (Figure 5B). The axoneme (0.53 ± 0.02 µm in diameter) of the sperm tail was surrounded with bilayered mitochondrial sheaths. The mitochondrial sheath was 1.27 ± 0.13 µm in diameter and retained a prominent gap (0.04 ± 0.01 µm) between its layers. The axoneme showed the typical '9 + 2' microtubular arrangement. Each outer microtubule was 0.07 ± 0.005 µm in diameter. The central two microtubules were surrounded by a membranous sheath 0.14 ± 0.02 µm in diameter (Figure 5C). The nucleus of the sperm was nearly 0.77 ± 0.07 µm in diameter and 2.20 ± 0.12 µm in length. The posterior part of the nucleus had a deep V-shaped fossa that housed the centriolar complex and acts as a socket for the neck region. The microtubules

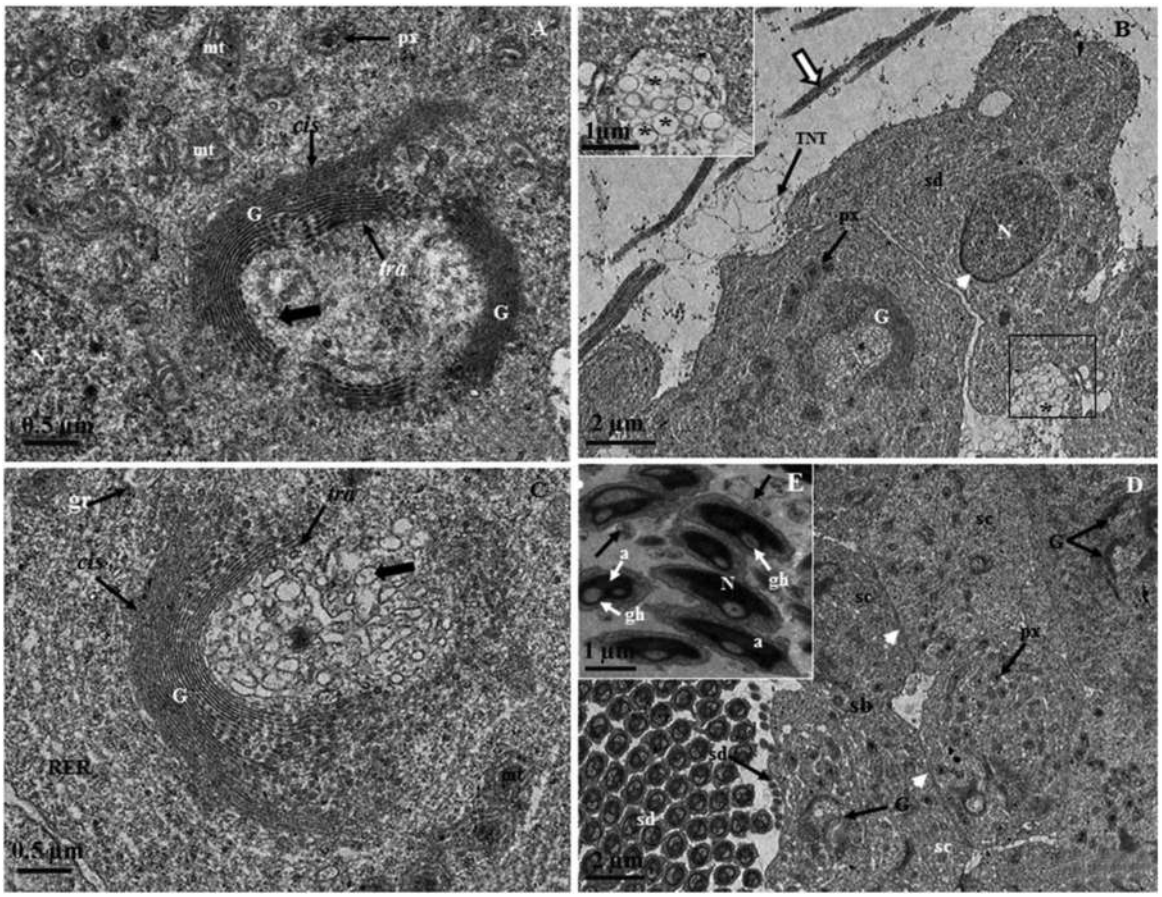

Figure 4. Transmission electron micrographs of ovotestis of smaller *L. alte* (0.46 ± 0.01 g). **A,** Enlarged view of part of a spermatocyte showing mitochondria (mt) of different shapes and sizes, stacks of Golgi complex (G). Note the small vesicles pinched off (bold arrow) from the trans-face (*tra*) of the Golgi complex. **B,** Condensation of nuclear materials on one side of inner nuclear wall of developing spermatid (white arrow head). Numerous secretory vesicles (*) of Sertoli cells are found very close to the developing spermatids. Inset: enlarged view of secretory vesicles of the marked area. Note the longitudinal section of many developing spermatids (bold arrow). **C,** Magnified view of Golgi complex (G) and rough endoplasmic reticulum (RER) of a developing spermatid. Numerous Golgi vesicles (bold arrow) are pinched off from the trans-face (*tra*) of Golgi complex in the developing spermatids. **D,** Spermatogenic cells arranged in a successive developmental state towards acinar lumen. Note the cell junctions (white arrow head) between spermatocytes. **E,** Manchette form of developing spermatids showing the lengthening of nucleus, development of glycogen helix (gh) and axoneme (a). The residual cytoplasmic material (RCM) buds off from the developing spermatids (black arrow). a—axoneme; *cis*—*cis*-face of Golgi complex; G—Golgi complex; gh—glycogen helix; gr—glycogen rosette; mt—mitochondria; N—nucleus; px—peroxisome; RER—rough endoplasmic reticulum; sb—syncytial bridge; sc—spermatocyte; sd—spermatid; *tra*—trans-face of Golgi complex; TNT—tunnelling nanotube.

of the axoneme emerged from this centriolar complex (Figure 5A).

Sertoli cells

The Sertoli cells were very irregular in structure and had no definite shape or size. These somatic cells were larger than spermatogenic cells and frequently observed (22 ± 8.09 in numbers per acinus) throughout the acinar space (Figures 2A–B). Two forms of the Sertoli cells can be distinguished based on their morphological characteristics and their locations in the acini of the ovotestis of *L. alte*: (i) cortical Sertoli (CrS) cells and (ii) luminal Sertoli (LmS) cells.

The CrS cells were larger (7.08 ± 1.03 µm in diameter) and located in the cortical compartment of the acini (Figures 2A–D, 2, 5D–E). A germinal epithelial layer was observed between CrS cells and the basal lamina of acini (Figures 2C–D and 3). Cells at the early stage of spermatogenesis such as spermatogonia and spermatocytes were developed as several cell clusters (or cell pyramids) over the CrS cells (Figures 2A–C). These spermatogenic cell clusters were semicircular or crescent-shaped measuring 2.04 ± 0.25 µm in height along their long axis and expanded laterally to approximately 3.59 ± 0.52 µm (Figure 2B). One part of the CrS cells was attached to the basal lamina of acini. Both the apical and lateral parts of the CrS cells had numerous tunnelling nanotubes (TNTs) of 6.72 ± 3.11 µm in length and 0.15 ± 0.13 µm in diameter (Figures 2B–D, 3, 5D). The TNTs of CrS cells (Figures 2B–D and 5D–E) were tapering and much longer than those of LmS cells (Figures 2B and 6A). In many ultrathin sections, the CrS cells appeared star-shaped due to the protrusions of their

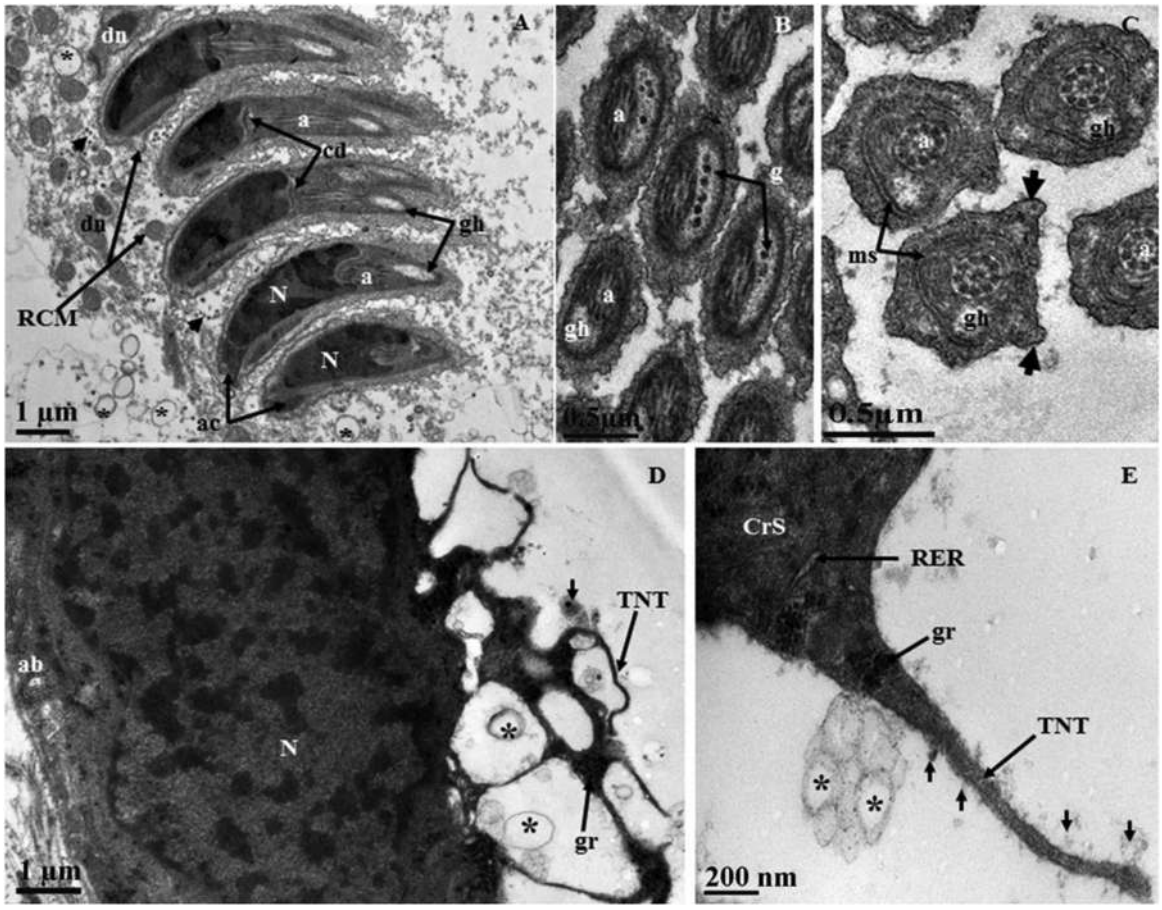

Figure 5. Transmission electron micrographs of ovotestis of smaller *L. alte* (0.46 ± 0.01 g). **A,** Longitudinal section of head of developing sperms inserted in a part of Sertoli cell which comprised numerous glycogen granules (arrowheads), electron-dense vesicles (dn) and secretory vesicles (*). Residual cytoplasmic material (RCM) is budded off from developing sperms. Note the development of acrosomal process (ac), glycogen helix (gh), axoneme (a) and centriolar derivative (cd) of sperms. **B,** Cross section of middle part of developing sperms near neck region displaying microtubular arrangement of axoneme (a) and glycogen helix (gh) including globular glycogen granules (g). **C,** Cross section of the tail portion of sperm showing double layered mitochondrial sheath (ms) around the axoneme (a) and glycogen helix (gh). Note the irregular lateral fins (arrow head) of the sperm's surface. **D,** Part of CrS cell showing its cytoplasmic constituents are transported to the acinar lumen through TNTs. Glycogen granules of CrS cell as a singlet (arrow head) or a cluster are moved through TNTs toward its distal end or acinar lumen. **E,** Enlarged view of TNT and its internal cellular components. Note the secretions of CrS cells transported (small arrows) to the lumen and the wall of TNT. ab–acinar boundary; asterisk (*)–secretory vesicles; CrS–cortical Sertoli cell; gr–glycogen rosette; N–nucleus; RER–rough endoplasmic reticulum; TNT–tunnelling nanotube.

cell surface TNTs and were surrounded by developing spermatogenic cells (Figure 3). Most TNTs of CrS cells penetrated between the developing spermatogonia (Figure 2C) and spermatocytes (Figures 2D and 3). The cytoplasm of CrS cells was deeply stained and comprised numerous mitochondria (0.51 ± 0.13 µm in diameter), rough endoplasmic reticulum (0.22 ± 0.07 µm in width of each cisternae), extensive glycogen granules, multiple electron-dense vesicles (0.22 ± 0.06 µm in diameter) and a few electron-lucent vesicles that measured 0.49 ± 0.04 µm in diameter (Figures 2C–D, 3,5A, 5D–E). Some cytoplasmic constituents such as vesicles and glycogen granules of the CrS cells were frequently found in the TNTs and might finally be released either to spermatogenic cells (Figures 2C and 3) or to the acinar lumen (Figures 3, 5A, 5D–E). The cytoplasmic components of CrS cells may help in the development of spermatogenic cells which were remote from the direct contacts of the Sertoli cells (Figures 4B and 5E). The glycogen granules in TNTs of CrS were transported either individually, measuring 0.03 ± 0.01 µm in diameter (Figure 5D) or as small clusters (36.55 ± 19.28 µm^2 in area) of glycogen granules (Figures 5D–E). The nucleus of the CrS cells was large (4.19 ± 0.16 µm in diameter) with a prominent nucleolus (1.28 ± 0.12 µm in diameter). The nucleoplasm was fibrous and granulated with electron-dense granules (Figures 3 and 5D).

The LmS cells were smaller (3.72 ± 0.13 µm in diameter) than CrS cells. LmS cells were mostly oval, pear-shaped or bell-shaped (Figures 2B and 6A–B) and located in the acinar medulla, free of the basal lamina of acini (Figure 1B). Developing spermatogenic cells, mainly spermatids, encircled the LmS cells (Figures 2B and 6A). The cytoplasm of LmS cells was

lightly stained and comprised of lysosomes (0.34 ± 0.07 µm in diameter), multiple stacks (0.47 ± 0.08 µm in diameter) of Golgi cisternae, rough endoplasmic reticulum (0.09 ± 0.03 µm in width) without definite shape, numerous cytoplasmic inclusions and a few glycogen granules (Figures 6A–C). Some developing spermatids were encircled with the cytoplasm of LmS cells that may help in transporting developing male gametes (Figure 6A). The TNTs of LmS cells were shorter (0.50 ± 0.24 µm in length) and blunt (0.25 ± 0.09 µm in thickness) than those of the CrS cells. These TNTs were connected to the adjacent developing spermatids directly or through the lateral fin of the spermatids (Figure 6A). Sertoli-Sertoli cell junctions and Sertoli-spermatogenic cell connections were found very frequently (Figures 2B, 3, 6A–B). The nucleus (5.15 ± 0.44 µm in diameter) was infrequently observed in the LmS cells and was mostly circular, with a small nucleolus measuring 0.35 ± 0.14 µm in diameter (Figures 2B and 6C).

Periacinar cells

The periacinar cells were narrow and elongated epithelial cells measuring 6.41 ± 0.41 µm in length and 1.08 ± 0.32 µm in width (Figure 6D). These cells were present in a discrete thin layer (3.32 ± 0.67 µm in thickness), tightly surrounding each acinus with several bundles (0.50 ± 0.16 µm in width) of collagen fibres (Figures 2C–D, 3, 6D). The cytoplasm of periacinar cells was comprised of Golgi complex, rough endoplasmic reticulum (each cisterna 0.06 ± 0.006 µm in width), numerous ribosome granules and several small secretory vesicles (Figures 7A–B). Some curls (0.14 ± 0.06 µm in diameter) of rough endoplasmic reticulum

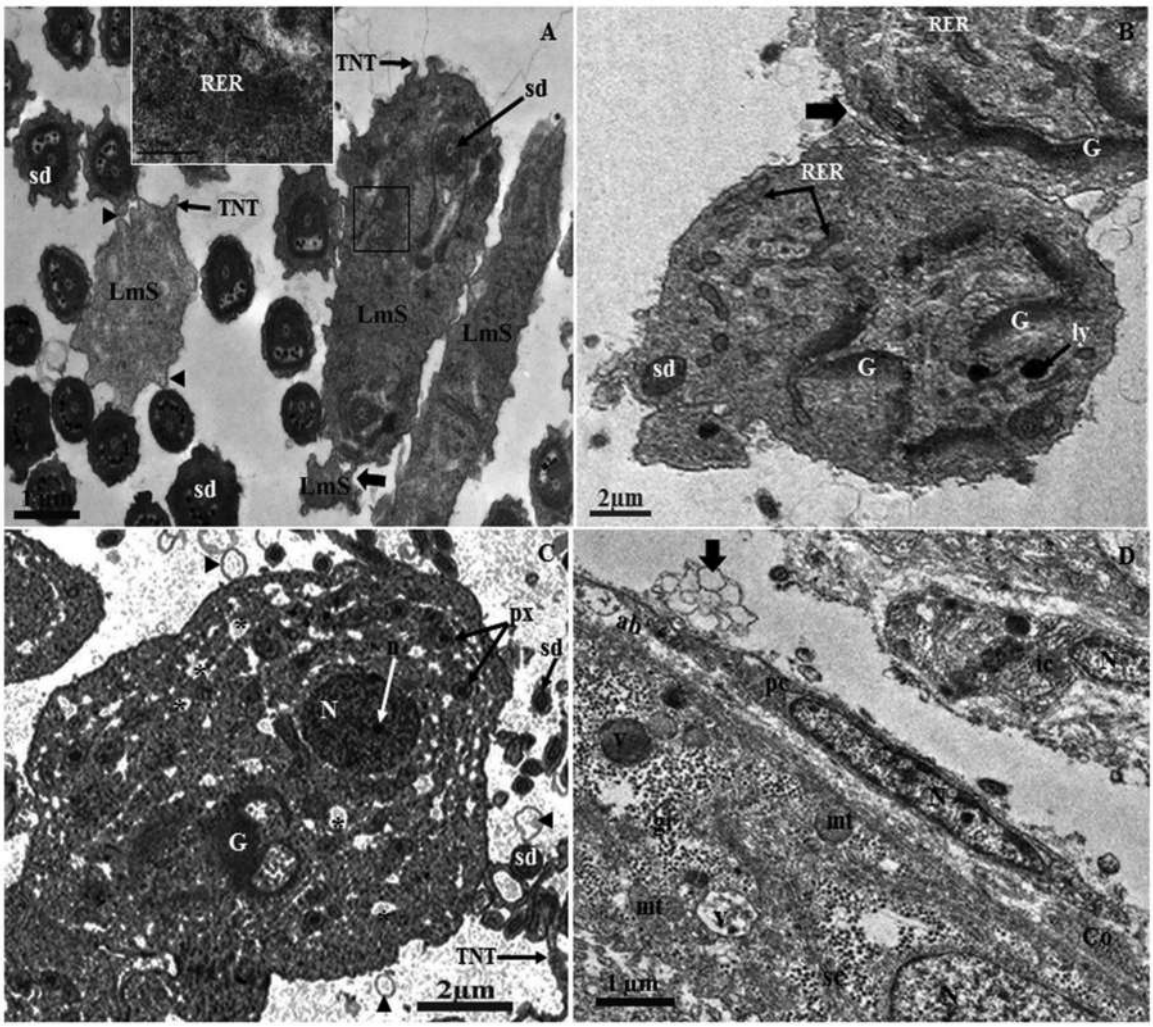

Figure 6. Transmission electron micrographs of ovotestis of smaller *L. alte* (0.46 ± 0.01 g). **A,** Arrangement of developing spermatids around the LmS cells of different shape and sizes. Enlarged view of the marked area in LmS cell is displaying rough endoplasmic reticulum (RER) in set. Note the Sertoli-Sertoli (bold arrow) and Sertoli-spermatids (arrowheads) junctions. **B,** Magnified view of LmS cells viewing several Golgi complexes, RER and lysosomes (ly). Bold arrow indicates Sertoli-Sertoli junction. **C,** The LmS cell showing numerous cytoplasmic inclusions (*), peroxisomes (px), Golgi complex (G) and a prominent nucleus (N). Multiple secretory vesicles (arrowheads) are secreted around the cell surface. **D,** Spatial arrangement of elongated periacinar cell (pc) and a part of interacinar cells (ic) in the interacinar zone. Note the cluster of secretory vesicles (bold arrow) very close to the layer of periacinar cells. ab–acinar boundary; Co–collagen fibres; G–golgi complex; gr–glycogen rosette; LmS–luminal Sertoli cell; mt–mitochondria; n–nucleolus; N–nucleus; pc–periacinar cell; sc–spermatocyte; sd–spermatid; TNT–tunnelling nanotubes; v–vesicle.

enfolded small amounts of cytoplasm (Figure 7A). The ribosome granules formed studs on the outer envelope of the nucleus and endoplasmic reticulum (Figures 7A–B). The nucleus of periacinar cells was slim and elongated measuring 4.91 ± 0.93 µm in length and 0.61 ± 0.23 µm in width. The periacinar cells were almost completely occupied by the nucleus which showed distinct double nuclear membranes (Figures 3,6C, 7A).

Interacinar cells

The interacinar cells were moderate in size and oval in shape, measuring 4.69 ± 1.37 µm in length and 2.20 ± 0.71 µm in width (Figures 2A–B, 6D, 7C–D). These cells were distributed commonly in the interacinar spaces, either singly or in a small group of cells, associated with many thin (0.04 ± 0.02 µm in diameter) muscle threads and some filamentous collagen fibres (Figure 7C). The cytoplasm of interacinar cells was composed of extensive rough endoplasmic reticulum (each cisterna 0.07 ± 0.02 µm in thickness), smooth endoplasmic reticulum, many lipid droplets (0.53 ± 0.17 µm in diameter), mitochondria, electron-dense vesicles (0.38 ± 0.14 µm in diameter), electron-lucent secretory vesicles (0.46 ± 0.20 µm in diameter) and numerous glycogen granules (Figures 6D and 7C–D). The outer wall of the endoplasmic reticulum was decorated with numerous ribosome granules (Figure 7D). Some cytoplasmic components of interacinar cells such as secretory vesicles, glycogen granules and lipid droplets were released outside the cell and distributed in the surroundings (Figures 7C–D). In some cases, the secretory vesicles form a cluster (approximately 1.25 ± 0.32 µm in diameter). They remain very close to the acinar outer wall and might be transported into the acini through the acinar boundary (Figure 6D). The nucleus of the interacinar cells was irregular in shape with a prominent double nuclear envelope.

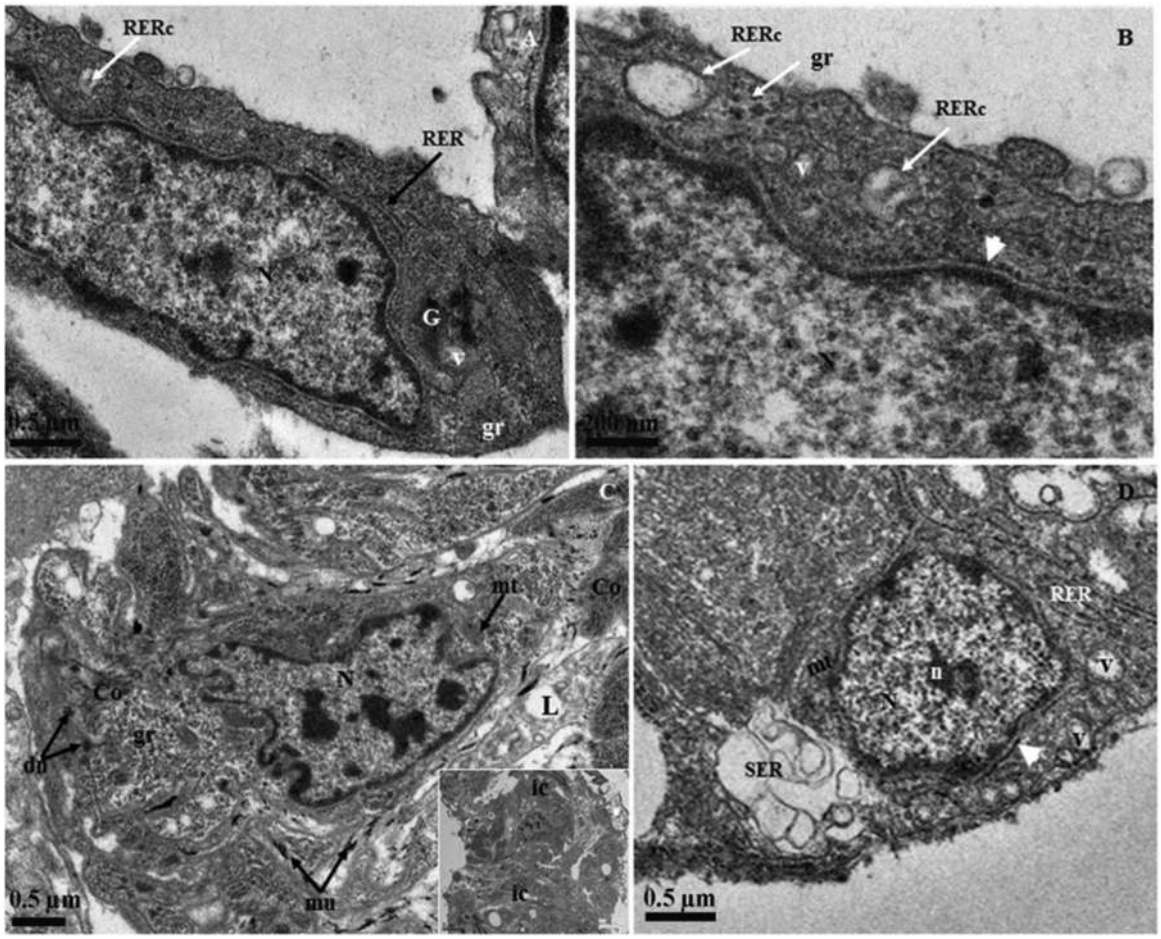

Figure 7. Transmission electron micrographs of ovotestis of smaller *L. alte* (0.46 ± 0.01 g). **A,** Part of periacinar cell displaying rough endoplasmic reticulum (RER), Golgi complex (G) and glycogen rosette (gr). **B,** Enlarged view of a part of periacinar cell showing many curls of RER studded with ribosome granules around a small part of cytoplasm. Note the decoration of ribosomes (white arrowhead) on the outer envelope of nucleus (N). **C,** Longitudinal section of an interacinar cell showing collagen fibres (Co) and some muscles (mu) around the cell. A small cluster of interacinar cells (ic) and their associated fibrous structures are shown in set. **D,** Cross section of an interacinar cell viewing double nuclear membrane decorated with ribosome granules (white arrowhead). dn–electron-dense vesicle; G–Golgi complex; gr–glycogen rosette; L–lipid droplets; mt–mitochondria; n–nucleolus; N–nucleus; RER–rough endoplasmic reticulum, RERc–curl of rough endoplasmic reticulum; SER–smooth endoplasmic reticulum, v–vesicle.

The nucleus was 3.23 ± 0.25 µm in length and 1.63 ± 0.49 µm in width (Figures 7C–D).

Oogenesis

The oogonia were very poorly developed, characterised by moderately electron-dense ooplasm with some lipid droplets (0.70 ± 0.13 µm in diameter) and had few mostly circular (0.29 ± 0.05 µm in diameter), mitochondria (Figure 8A). Semithin sections revealed that the oogonium was elongated approximately 1.09×0.21 µm in size and always located in the cortical area of acini (Figure 2A). The follicle cell layer was thin (0.30 ± 0.06 µm in thickness), tightly encircled the oogonia and was separated from developing male gametes in the acinus (Figures 2A and 8A–B). The follicular cleft was not developed between oogonia and the layer of follicle cells (Figures 2A and 8A). It was sometimes found that parts of the LmS cells were located between developing spermatogenic cells and the follicle cell layer (Figure 8B).

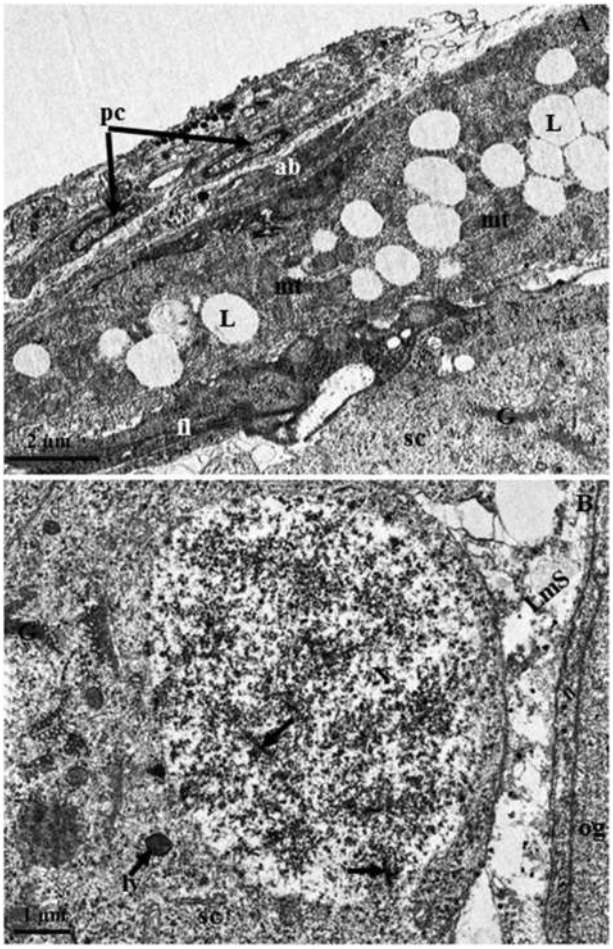

Figure 8. Transmission electron micrographs of ovotestis of smaller *L. alte* (0.46 ± 0.01 g). **A,** An oogonium showing its ooplasm includes some mitochondria (mt) and lipid droplets (L). The oogonium is tightly surrounded by follicular layer without follicular cleft. **B,** The LmS cell intermingled with follicular layer (fl) and helping to separate male and female gametes in the acini. Note the prominent chromatin threads (arrow) in nucleoplasm of the spermatocyte (sc). G–stacks of Golgi apparatus; L–lipid droplets; ly–lysosome; N–nucleus; og–oogonium; pc–periacinar cell; sc–spermatocyte.

Ovotestis of larger L. alte

The acini (7.71 ± 0.78 µm in diameter) were larger and slightly more elongated than those of smaller slugs. The acinus had only a few developing spermatogenic cells and only one developed oocyte with various cell organelles (Figures 9A–D and 10A–D). The acinar boundary near the oocyte was slightly thinner (0.73 ± 0.16 µm) whereas the thickness of rest of the acinar boundary was almost the same as in smaller slugs (1.21 ± 0.1 µm).

Spermatogenesis

Spermatogonia were either absent or very much less frequent in almost all acini. Serial semi-thin sections revealed that a large part of the acini was occupied by a larger oocyte. As a result, the overall numbers of spermatogenic cells in the acini of larger slugs were lower than in smaller slugs (Figure 9A). The morphological features of developing male gametes in the acini of larger slugs resembled those of smaller slugs (Figures 9A–C).

Sertoli cells

Small numbers of Sertoli cells were found atrophied or as residual cellular fragments in the acini of larger *L. alte* (Figure 9A). The (LmS) cells were smaller (0.33 ± 0.06 µm in diameter), that is, 1/10 of the size of those of smaller slugs. The LmS cells were more common than CrS cells in the acini (Figure 9A). The CrS cells (0.36 ± 0.04 µm in diameter) were very indistinct and had lost their attachment to the basal lamina of acini. The development of cell surface TNTs of Sertoli cells was significantly less (Figure 9A). A number of large vacuoles (2.58 ± 0.70 µm in diameter) were observed in the LmS cells. These vacuoles may have been formed by release or phagocytosis of mature sperms (Figure 9D). In some ultrathin sections, it was found that various cytoplasmic components of LmS cells had emerged into the acinar lumen due to disintegration of the cell (Figure 10B).

Periacinar cells

The characteristics of the periacinar cells in older slugs were similar to those of the smaller slugs. There were few periacinar cells in the ovotestis of larger slugs (Figure 9B).

Interacinar cells

Interacinar cells were either absent or very low in numbers in the interacinar spaces of the ovotestis of larger slugs (Figure 9A). However, their cellular features were identical to those of the smaller slugs. In some

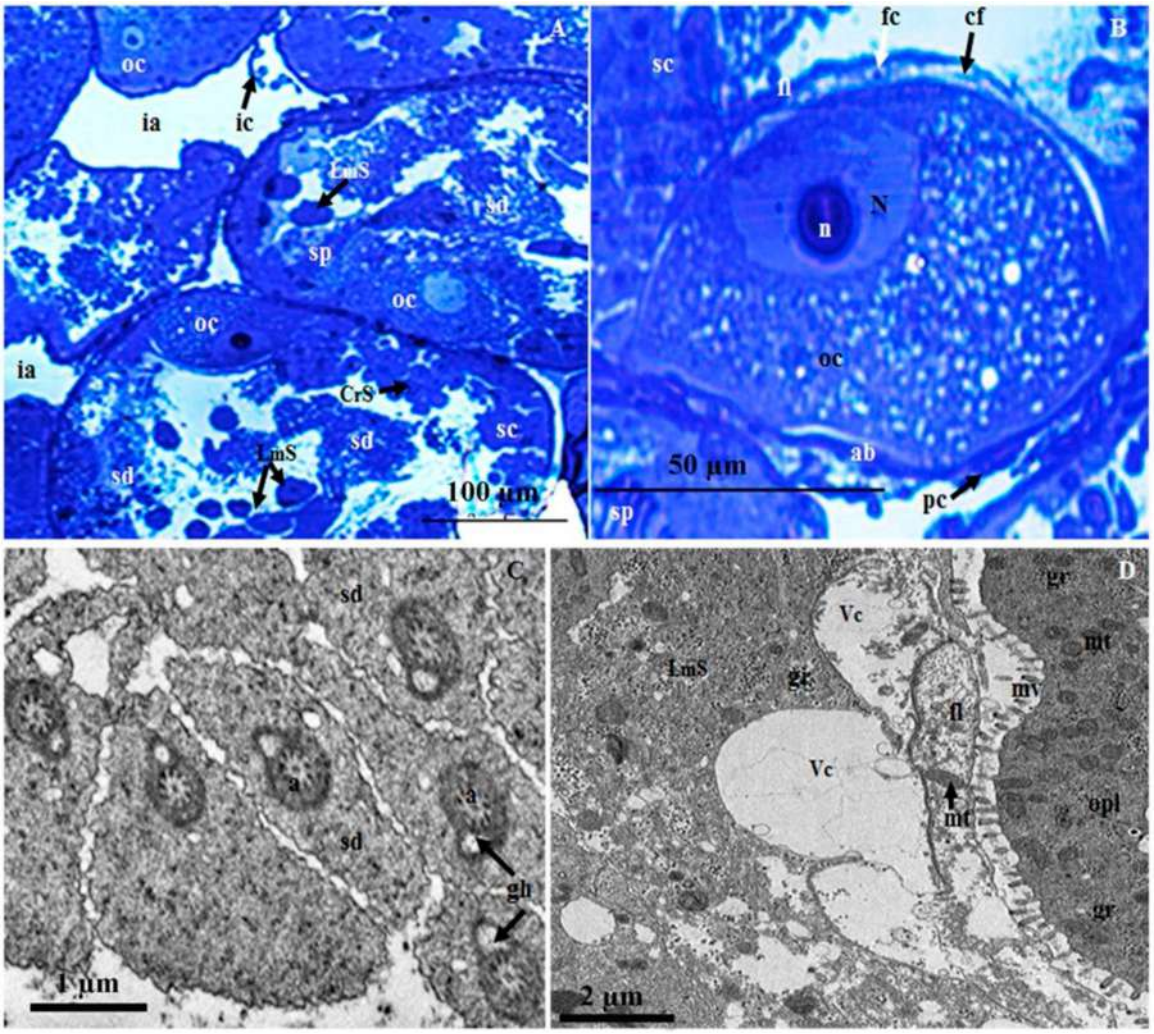

Figure 9. Ovotestis of larger *L. alte* (1.06 ± 0.118 g). **A–B,** Semithin sections. A, Acinus showing only one vitellogenic oocyte (oc) with some spermatogenic cells. Interacinar space (ia) comprised of a very small number of interacinar cells (ic) or none. B, Magnified view of the oocyte with prominent nucleus (N) and nucleolus (n). The oocyte is surrounded by a follicular layer (fl) with a well-developed follicular cleft (cf). **C–D,** Transmission electron micrographs. C, A part of acinus showing developing spermatids (sd) identical to those of smaller slugs. D, Sertoli cell with large cytoplasmic vacuoles (Vc) and some small glycogen rosettes (gr). a–axoneme; ab–acinar boundary; CrS–cortical Sertoli cell; fc –follicular cell; fl –follicular layer; gh–glycogen helix; L–lipid droplets; LmS–luminal Sertoli cell; mt–mitochondria; mv–microvilli; Om–oolemma; opl–ooplasm; sd–spermatid; sp–sperm.

cases, the interacinar zones lacked interacinar cells (Figure 9A).

Oogenesis

Each acinus was composed of only one vitellogenic oocyte (Figures 9A–B). Semithin sections revealed that the oocyte was usually oval in shape and approximately 4.91 × 3.39 µm in size (Figures 9A–B). One part of the oocyte was closely attached to the inner wall of the acinar boundary (Figures 9B and 12B). The oocytes were surrounded by a layer of follicle cells (Figures 9A–B, 10, 11D, 12B). Vitellogenic oocytes were characterised by a foamy appearance due to the presence of various electron-lucid and electron-dense bodies in the ooplasm (Figures 9A–B and 10). The ooplasm comprised rough endoplasmic reticulum (0.07 ± 0.03 µm width of each cisterna), several mitochondria, glycogen rosettes (0.47 ± 0.17 µm in diameter), numerous lipid droplets and electron-dense yolk granules (Figures 9D and 10A–D). The yolk granules were formed of intermediate (or immature) yolk granules of different shapes and sizes. The intermediate yolk granules were apparently produced by continuous coalescence of small yolk precursors and lipid droplets (Figures 10A–D). The mitochondria were circular (0.23 ± 0.04 µm in diameter) or elongated (approximately 0.38 × 0.16 µm) in shape. Some mitochondria were arranged in a single file around the nuclear membrane (Figure 10C). The nucleus (1.97 ± 1.2 µm in diameter) of the oocyte was large and circular in cross section. The nucleoplasm included distinct chromatin fibres and a prominent nucleolus (Figure 10C). The nucleolus (0.60 ± 0.49 µm in diameter) was composed of moderately electron-dense, finely granulated, plasma-like intranucleolar materials (Figure 10C). The nucleoplasm and ooplasm was demarcated

by the nuclear membrane with prominent nucleopores (Figure 10C). The luminal face of the oolemma was composed of numerous microvilli, approximately 0.25 × 0.05 µm in size. The tips of the microvilli with electron-dense granules leaned into the follicular cleft and supported the endocytosis of yolk precursors as an exogenous source of yolk synthesis (Figures 9D and 10A–B).

Follicle cell layer

The follicle cell layer consisted of a few flattened follicle cells 1.61×0.75 µm in size (Figure 10B). This layer formed a barrier around each developing female gamete and isolated it from developing male gametes (Figures 9B and 10A–B). The follicular layer (0.72 ± 0.12 µm in width) was thicker around vitellogenic oocytes than oogonia. A prominent follicular cleft or cavity (0.46 ± 0.26 µm in width) was formed at the apical and lateral side of the oocyte (Figures 9B, 9D, 10A–B). The follicular cleft was filled with electron-dense granules and secretory vesicles measuring 0.14 ± 0.07 µm in diameter (Figures 9D and 10A–B). The follicular layer was thin (0.18 ± 0.07 µm in width) and lay between the oolemma and the wall of the acinar boundary (Figure 10D). The follicle layer consists of mitochondria, numerous small vesicles and abundant glycogen rosettes (Figures 9D and10A–B). The glycogen rosettes in the follicular layer were smaller than those in the ooplasm or Sertoli cells (Figures 9D and 10B).

The characteristics of major structures in both smaller and larger *L. alte* are summarised in Table 1. A comparative diagram of acini in the ovotestis of both smaller and

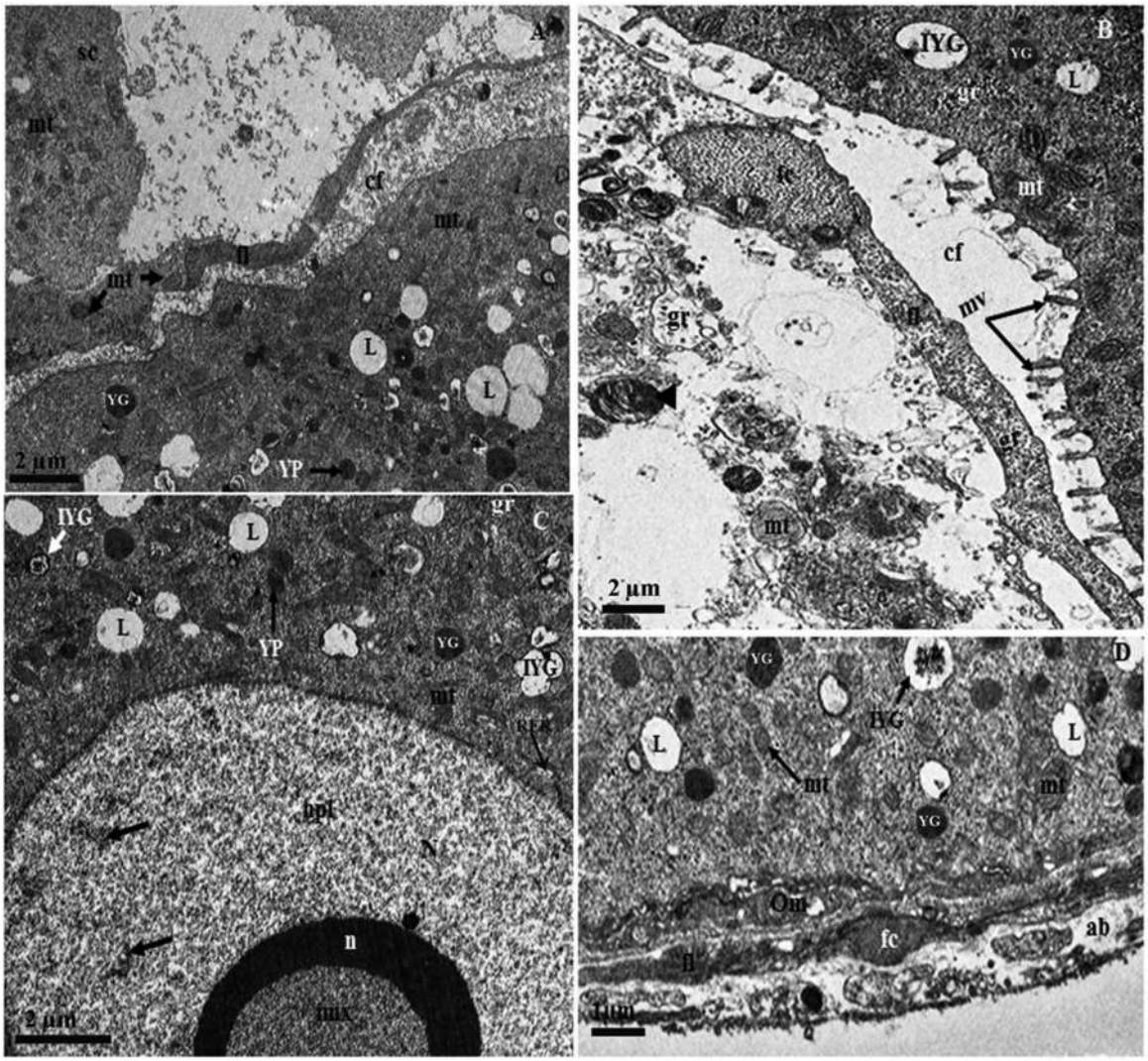

Figure 10. Transmission electron micrographs of a part of acinus of larger *L. alte* (1.06 ± 0.118 g). **A,** An irregular follicular layer (fl) and follicular cleft (cf) over the apical part (luminal face) of oolemma (Om). **B,** Part of follicular layer (fl) with a prominent follicle cell (fc). Note the various components of residual part of LmS cell near the follicular layer. Arrowhead–distorted mitochondria. **C,** Some mitochondria (mt) are arranged in a single file around the nuclear membrane. Note the nucleoplasm (npl) consists of some chromatin fibres (arrows) and the nucleolus (n) comprised of intranucleolar matrix (imx). **D,** Part of oocyte showing the organisation of thin follicular layer (fl) between oolemma (Om) and acinar boundary (ab). ab–acinar boundary; fc–follicle cell; fl–follicular layer; gr–glycogen rosette; IYG–intermediate yolk granule; L–lipid droplet; mt–mitochondria; mv–microvilli; Om–oolemma; RER–rough endoplasmic reticulum; YG–yolk granule; YP–yolk precursor.

Table 1. Comparison of the major characteristics of ovotestis of smaller (0.46 ± 0.01 g) and larger (1.06 ± 0.118 g) *L. alte* (Férussac, 1822).

Characteristics of ovotestis	Smaller slug*	Larger slug
1. Spermatogonia	+++	–
2. Spermatocytes	+++	++
3. Spermatids	+++	++
4. Sperms	+++	++
5. Periacinar cells	+++	++
6. Interacinar cells	+++	ɣ
7. Cortical Sertoli (CrS) cells	+++	ɣ
8. Luminal Sertoli (LmS)cells	+++	++
9. Tunnelling nanotubes (TNTs)	+++	ɣ
10. Oogonia	+	–
11. Vitellogenic oocyte	ɣ	+
12. Microvilli on oolemma	ɣ	+++
13. Distribution of yolk granules in ooplasm	ɣ	+++
14. Follicle cells in follicular layer	–	+++
15. Thickness of follicular layer	–	+++
16. Follicular cleft	–	+++

* (–) absent; (+) present; (ɣ) few in number (or thin); (++) moderate in number; (+++) high in number (or thick).

larger *L. alte* is presented in Figure 11. Comparative cell size relationships of the different gametogenic cells and the somatic cells in the ovotestis of smaller and larger slugs are documented in Figure 12.

Discussion

The gradual increase of VSI with an increase in body weight may be the result of growth of the albumen gland and acumulation of its constituents (e.g., vitellogenin, ferritin, etc.). The gradual decrease of VSI in the larger slugs (0.83–2.1 g) might be due to the expenditure of the vitellogenin/ferritin of the albumen gland in oogenesis in the acini. It may be presumed that the low VSI in smaller slugs is an indication of functional spermatogenesis and the higher value of VSI in larger individuals is suggestive of the proliferation of oogenesis, as reported in other systellommatophoran slugs (Bing *et al*. 2008; Roy *et al*. 2018).

Gametogenesis

The present study describes the fine structural details of the ovotestis of *L. alte* of different body weight classes, relative to other terrestrial and aquatic pulmonate molluscs. The overall characteristics of different stages of gametogenesis in *L. alte* are mostly similar to other terrestrial (Quatrini and Lanza 1965; Nagabhushanam and Kulkarni 1971; Kulkarni 1973; Rakshit *et al*. 2005; Roy *et al*. 2016) and aquatic pulmonate molluscs (Jong-Brink *et al*. 1976, 1977; Bing *et al*. 2008; Silva *et al*. 2009; Roy *et al*. 2018). The body weight of *L. alte* is directly correlated to the proliferation of either spermatogenesis or oogenesis in the respective ovotestis as reported in other hermaphrodite pulmonates (Sabelli and Sabelli 1980; Tomiyama 1995; Ohbayashi-Hodoki *et al*. 2004; Hermann *et al*. 2009; Nakadera *et al*. 2015; Roy *et al*. 2016, 2018).

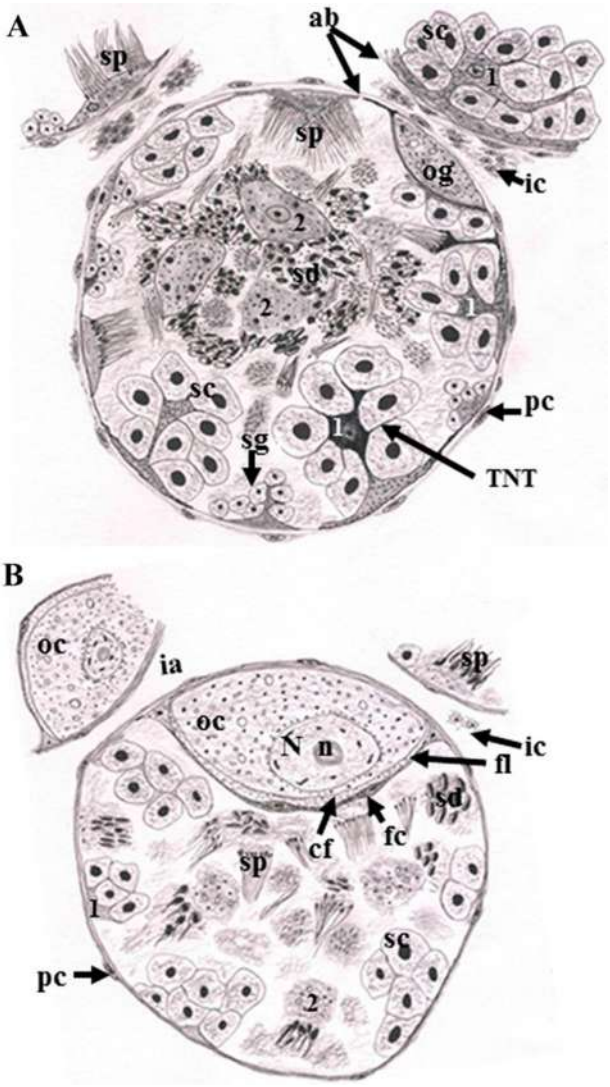

Figure 11. Diagrammatic representations of acini in the ovotestes of both smaller (**A**) and larger (**B**) *L. alte* showing an acinus and its allied structures. Note the cell pyramid of developing spermatogenic cells on and around the Sertoli cells. ab–acinar boundary; cf–follicular cleft; fc–follicle cell; fl–follicular layer; ia–interacinar space; ic–interacinar cell; n–nucleolus; N–nucleus; pc–periacinar cell; sc–spermatocyte; sg–spermatogonia; sd–spermatid; sp–sperm; TNT–tunnelling nanotubes; 1–cortical Sertoli cell; 2–luminal Sertoli cell.

The acini of *L. alte* with relatively lower body weight, presumably younger slugs, have enhanced spermatogenesis and presumably act as males (Roy *et al*. 2016, 2018). Oogenesis is increased in the acini of the individuals of larger body weight, apparently older slugs, and follows resource allocation principles (Bateman 1948; Charnov 1996; Leonard 2005). Larger resources are required to develop female gametes than male gametes (Ohbayashi-Hodoki *et al*. 2004; Norton and Bronson 2006). Smaller slugs have fewer resources, and produce mostly male gametes, whereas larger individuals possess larger resources and produce mostly female gametes. As a result individual slugs can function as potential sperm donor and sperm recipient during copulation at different stages of their

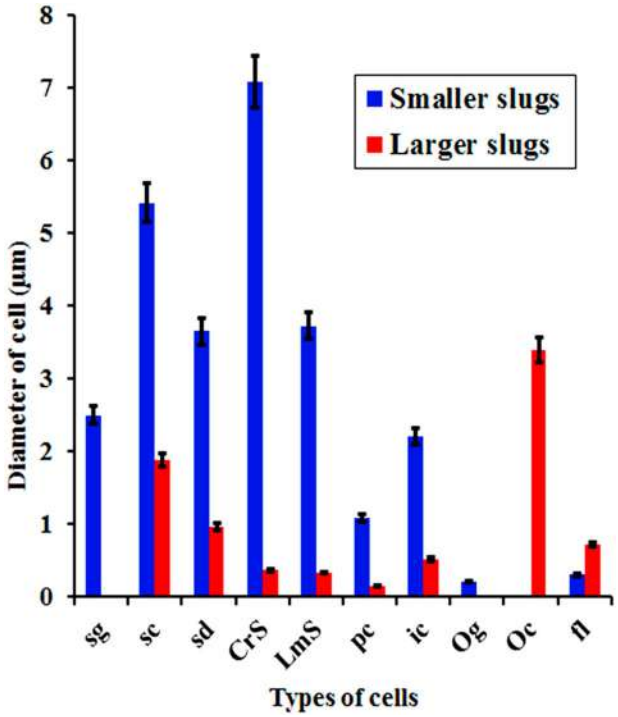

Figure 12. Histogram showing the cell size relationship of different gametogenic and somatic cells in the ovotestes of smaller (0.46 ± 0.01 g) and larger (1.06 ± 0.118 g) *L. alte*. The thickness of the follicular layer is also compared. N = 3. Abbreviation: CrS–cortical Sertoli cell; fl–follicular layer; ic–interacinar cell; LmS–luminal Sertoli cell; pc–periacinar cell; sc–spermatocyte; sg–spermatogonia (absent or very rarely found in larger slugs); sd–spermatid; Oc–oocyte (only found in larger slugs); Og–oogonium (only found in smaller slugs).

development (Tomiyama 1995; Ohbayashi-Hodoki *et al*. 2004; Jordaens *et al*. 2005; Hermann *et al*. 2009; Nakadera *et al*. 2015).

The spermatogenic cells of *L. alte* are successively arranged on the basal lamina of acini according to their maturation; i.e., more mature spermatogenic cells are usually found near the acinar lumen, which is similar to other pulmonate molluscs (Jong-Brink *et al*. 1977; Rakshit *et al*. 2005; Bing *et al*. 2008; Roy *et al*. 2016, 2018). The vesicles of different forms in developing spermatogenic cells morphologically and morphometrically resemble those of the CrS cells. We speculate that these vesicles are transported from CrS cells to the spermatogenic cells and assist in their gametogenic development. The axonemal microtubules in the manchette form of developing spermatids are arranged in such a way that they help transform spherical cells to elongated spiral cells with a cytoskeletal support (Okamura and Nishiayama 1976). Additionally, the helical compartment containing glycogen granules and the mitochondrial sheath are formed during the manchette formation. It has previously been observed that glycogen synthesis and its accumulation within the glycogen helix occurred in late spermatids or developing spermatozoa (Anderson and Personne 1967, 1970; Healy 2001). It is assumed that the large amount of glycogen stored in the developing sperms may provide nutrition and the mitochondrial sheaths around the axoneme may help in their motility (Buckland-Nicks 1998; Healy 2001; Till-Bottraud *et al*. 2005). Some residual cytoplasmic material (RCM) was budded off from the developing spermatids during spermatogenesis to achieve their typical elongated, slender shape as described in other molluscs (Tokuyasu *et al*. 1972; Jong-Brink *et al*. 1977). The RCM is phagocytised by Sertoli cells (Jong-Brink *et al*. 1977). The acrosomal process, which may be species-specific in other gastropods (Jong-Brink *et al*. 1976, Rigby 1982), is small in *L. alte*, has a prominent notch at the proximal end and is located on the upper or lateral side of the nucleus at the anterior of the developing spermatids.

The acinus of larger *L. alte* has only one vitellogenic oocyte, as reported in other terrestrial hermaphrodite pulmonates (Parivar 1978; Griffond and Bolzoni-Sungur 1986; Boato and Rasotto 1987; Horn *et al*. 2005; Rakshit *et al*. 2005; Silva *et al*. 2009; Roy *et al*. 2016). The oocytes contain mitochondria, rough endoplasmic reticulum, glycogen rosettes and lipid droplets similar to other molluscs, and are involved in auto-synthetic yolk formation (Terakado 1974; van der Wal 1974). Heterosynthetic yolk formation is accomplished by a endocytosis of exogenous yolk precursors through the oolemma of the vitellogenic oocyte (Jong-Brink *et al*. 1976; Eckelbarger and Blades-Eckelbarger 1989). The yolk formation appears to be continuous throughout the oogenesis of *L. alte* and occurs through the gradual coalescence of different yolk precursors as

reported in other pulmonate molluscs (Favard and Carasso 1958; Jong-Brink *et al*. 1976; Roy *et al*. 2018). Female specific secretions of the oocytes may inhibit the development of spermatogenesis, and as a result the growth of spermatogenic cells and associated somatic cells are suppressed in the ovotestis of larger *L. alte*.

Veronicellidae (e.g., *L. alte*) and Onchidiidae (e.g., *O. tigrinum*) are members of the monophyletic group Systellommatophora which is the sister group of Stylommatophora (including Achatinidae, e.g., *A. fulica,* and Ariophantidae, e.g., *M. indica*) (Bouchet and Rocroi 2005; Jörger *et al*. 2010). The structural characteristics of the ovotestis of *L. alte* are closer to those of other terrestrial Stylommatophora (Griffond and Bolzoni-Sungur 1986; Tomiyama 1996; Rakshit *et al*. 2005; Roy *et al*. 2016) than to those of the aquatic Systellommatophora (Deshpande and Nagabhushanam 1983; Bing *et al*. 2008; Roy *et al*. 2018) or the aquatic pulmonate Hygrophila (Joosse and Reitz 1969; Jong-Brink *et al*. 1976, 1977). The acinus of *L. alte* contains only one vitellogenic oocyte, as is the case in other terrestrial pulmonate molluscs (Parivar 1978; Tompa 1984; Griffond and Bolzoni-Sungur 1986; Boato and Rasotto 1987; Horn *et al*. 2005; Rakshit *et al*. 2005; Silva *et al*. 2009; Roy *et al*. 2016). Roy *et al*. (2018) tabulated (*cf*. Table 2) the available results on the gametogenesis of pulmonate molluscs and proposed that the number of oocytes in each acinus primarily depends on the corresponding habitats of the pulmonate species rather than their taxonomic relatedness.

Gonadal somatic cells

There are four types of gonadal somatic cells in *L. alte*: Sertoli cells, follicle cells, periacinar cells and interacinar cells. In the acini, the Sertoli cells are spermatogenesis-specific while follicle cells are oogenesis-specific, as is also reported in other pulmonate molluscs (Griffond and Bolzoni-Sungur 1986; Eckelbarger and Blades-Eckelbarger 1989; Rakshit *et al*. 2005; Roy *et al*. 2016, 2018). The cytoplasm of the gonadal somatic cells comprises a large number of glycogen granules and secretory vesicles which may indicate that they are associated with nutrition (Barth and Jansen 1960, 1961, 1962; Quatrini and Lanza 1965; Starke 1971; Jong-Brink *et al*. 1977; Roy *et al*. 2016, 2018) and some hormonal functions (Lofts and Bern 1972; Parivar 1980).

It is described here for the first time that the Sertoli cells of *L. alte* include two varieties, CrS cells and LmS cells, differentiated by their location in the acini and morphological features. All Sertoli cells possess several tunnelling nanotubes (TNTs) on their free (luminal) cell surface. The TNTs of CrS cells are comparatively tapering and much longer than those of LmS cells which may possibly facilitate their penetration between developing spermatogenic cells. The TNTs create a thin cytoplasmic bridge between nutritive Sertoli cells and developing spermatogenic cells which do not have direct contact with them (Roy *et al*. 2016, 2018). The TNTs transport cellular components of Sertoli cells into the developing spermatogenic cells (Rustom *et al*. 2004). The Sertoli cells are known to act as secretory cells (Barth and Jansen 1960; Quatrini and Lanza 1965; Starke 1971; Jong-Brink *et al*. 1977) but there is uncertainty about their steroid producing properties in molluscs (Lofts and Bern 1972; Jong-Brink *et al*. 1977, 1981; Parivar 1980). In the present study, the LmS cells of *L. alte* comprised several membrane-bound secretory products that may be suggestive of some hormonal function but this requires further investigations. Several large vacuoles are found in the cytoplasm of LmS cells in larger *L. alte*, presumably formed after phagocytosis of residual sperms or residual cytoplasmic material of developing spermatids (Jong-Brink *et al*. 1977). In smaller *L. alte*, several developing spermatogenic cells are found in the cytoplasm of the LmS cells and we assume that these cells may be involved in the transportation of spermatogenic cells. Earlier reports have described the involvement of Sertoli cells in compartmentalisation between male and female gametes in the acini of some pulmonates such as *Archachatina marginata* (Swainson, 1821) (Odiete 1982), *Levantina hierosolyma* (Mousson, 1854) (O'Donovan and Abraham 1987) but in the present study it is observed that the Sertoli cells of *L. alte* are not directly involved in the formation of any significant compartment or layer between male and female gametes, corroborating findings for some other pulmonates (Rakshit *et al*. 2005; Roy *et al*. 2016, 2018). The cytoplasm of Sertoli cells in larger *L. alte* had low volumes of cell organelles possibly due to these cells' lesser activity (Parivar 1980) in this stage of development in the ovotestis where oogenesis is the prime process (Roy *et al*. 2018).

In *L. alte*, the follicle cells are arranged in a layer and completely surround the oocyte, which has one end attached to the acinar boundary. The follicular layer between the acinar boundary and oocyte of *L. alte* is very thin and covers the basal side of the oocyte more tightly than its apical side, possibly providing a mechanical support to ensure proper development. In some pulmonates, the follicular layer covers only the apical part of the oocyte (Jong-Brink *et al*. 1976; Griffond and Bolzoni-Sungur 1986). Possibly, the wrapping of the oocyte in the acinus by the follicular layer may be species-specific (Coggeshall 1972; Jong-Brink *et al*. 1976; Griffond and Bolzoni-Sungur 1986; Roy *et al*. 2016, 2018). The follicular layer is well developed in vitellogenic oocytes and has a prominent cleft. The development of this cleft is directly correlated to the growth of the female gamete (Jong-Brink *et al*. 1976). The follicular layer in *L. alte* consists of various proteosynthetic organelles, glycogen granules, different electron-dense

granules and secretory vesicles that are secreted in the follicular cleft or cavity and may act as an exogenous source of yolk precursors. The electron-dense granules in the follicular cleft congregated at the distal end of the microvilli of the oolemma of oocytes. It is assumed that the microvilli of oocytes in the ovotestis of *L. alte* are strongly involved in the endocytosis of yolk precursors as reported in other molluscs (Taylor and Anderson 1969; Coggeshall 1972; Jong-Brink *et al*. 1976; Eckelbarger and Blades-Eckelbarger 1989). The follicular layer is involved in the compartmentalisation of ovotestis in *L. alte* for individual development of male and female gametes as reported in other hermaphrodite molluscs (Luchtel 1972a, b; Jong-Brink *et al*. 1983; Bing *et al*. 2008; Roy *et al*. 2016, 2018).

The periacinar cells are distributed in a discrete thin layer around each acinus of *L. alte*. The cells structurally resemble the mammalian myoid cells around the seminiferous tubules (Skinner and Fritz 1985; Beguelini *et al*. 2013; Roy *et al*. 2016, 2018). Like peritubular myoid cells, the periacinar cells may promote the release of mature sperms into the acinar lumen and subsequently the acinar duct through their secretions and peristaltic waves (Maekawa *et al*. 1996; Roy *et al*. 2016, 2018). The periacinar cells are few in number in the ovotestis of the older (larger) slugs where oogenesis is prominent, similar to other hermaphrodite pulmonates (Roy *et al*. 2016, 2018).

The interacinar cells of *L. alte* are secretory cells frequently observed in the smaller slugs, and fundamentally resemble vertebrate interstitial cells. In the interacinar space these cells are usually found as a small cluster of cells, associated with collagen fibres and some muscles. It is assumed that like vertebrate interstitial cells, the interacinar cells may function in male-specific steroid hormone production. The transmission electron microscopic (TEM) observations suggest that the growth of somatic cells in the ovotestis of *L. alte* are gametogenesis specific and may have some role in the production of proteins and steroids as reported earlier in other pulmonates (Lofts and Bern 1972; Parivar 1980). In some cases, it is found that small clusters of electron-lucent secretory vesicles accumulated very close to the acinar wall in smaller slugs. These may facilitate uptake of the secretory materials of the interacinar cells into acini and promote spermatogenesis. In larger *L. alte*, the development of oogenesis and higher production of female-specific hormones may repress the growth of interacinar cells. As a result the populations of these cells are much lower in the interacinar zones of the ovotestis (Roy *et al*. 2018). The copulation of different body weight class individuals of *L. alte* is probably mediated by one of the internal signals of proliferation of specific gametogenesis (Table 1) in the ovotestis of respective individuals as reported in other pulmonates (Ohbayashi-Hodoki *et al*. 2004).

Acknowledgments

The authors express their thanks to the Department of Zoology, City College, Kolkata for their necessary help in light microscopic study and to the staff of TEM unit, Department of Anatomy, AIIMS New Delhi for their technical support and photographic services. The authors thank Dr. Amit Mukherjee and all other faculty members, Mollusca Section, Zoological Survey of India, India, for identification of specimens. The authors also express their thanks to the Head of the Department of Zoology and other faculty members of West Bengal State University, Barasat, West Bengal, India. The authors are also grateful to the reviewers of the manuscript for their constructive suggestions.

Disclosure statement

No potential conflict of interest was reported by the authors.

References

Anderson, W.A. & Personne, P. (1967) The fine structure of the neck region of spermatozoa of *Helix aspersa*. *Journal de Microscopie* 6, 1033–1042.

Anderson, W.A. & Personne, P. (1970) The localization of glycogen in the spermatozoa of various invertebrate and vertebrate species. *The Journal of Cell Biology* 44, 29–51.

Angeloni, L. & Bradbury, J. (1999) Body size influences mating strategies in a simultaneously hermaphroditic sea slug, *Aplysia vaccaria*. *Ethology Ecology and Evolution* 11, 187–195.

Barth, R. & Jansen, G. (1960) Über den begriff "Kinoplasma" in der Spermiogenese von *Australorbis glabrata olivaceus* (Mollusca, Pulmonata, Planorbidae). *Memórias do Instituto Oswaldo* Cruz 58, 209–228.

Barth, R. & Jansen, G. (1961) Über die Formver*änderungen des Golgi-Apparates während* der Spermiogenese von *Australorbis glabratus olivaceus* (Mollusca, Pulmonata, Planorbidae). *Memórias do Instituto Oswaldo* Cruz 59, 83–114.

Barth, R. & Jansen, G. (1962) Beobachtungen fiber die Entwicklung und Ernährung der Eizellen yon *Australorbis glabratus olivaceus* (Gastropoda, Pulmonata, Planorbidae). *Anais da Academia Brasileira de* Ciências 34, 381–389.

Bateman, A.J. (1948) Intra-sexual selection in *Drosophila*. *Heredity* 2, 349–368.

Beguelini, M.R., Taboga, S.R. & Morielle-Versute, E. (2013) Ultrastructural characteristics of the spermatogenesis during the four phases of the annual reproductive cycle of the black Myotis bat, *Myotis nigricans* (Chiroptera: Vespertilionidae). *Microscopy Research and Technique* 76, 1035–1049.

Bhavare, M.K. & Magare, S.R. (2017) Ecology and population studies of land slug, Laevicaulis alte in Shahada region. *Journal of Applied and Advanced Research* 2, 63–66.

Bing, H.U., Xiao-zhen, Y., Xu-gan, W.U., Wei-ming, T. & Yong-xu, C. (2008) Development of gonad in different body weights of *Onchidium struma*. *Zoological Research* 29, 145–151.

Bluemink, J.G. (1967) The subcellular structure of blastula of *Lymnaea stagnalis* L. (Mollusca) and the mobilization of the nutrient reserve. Ph.D. Thesis, University of Utrecht.

Boato, A. & Rasotto, M.B. (1987) Functional protandry and seasonal reproductive cycle in *Solatopupa similis* (Bruguière) (Pulmonata Chondrinidae), *Bolletino di zoologia* 54, 119–125.

Bouchet, P. & Rocroi, J-P. (2005) Classification and nomenclator of gastropod families. *Malacologia* 47, 1–397.
Buckland-Nicks, J. (1998) Prosobranch parasperm: sterile germ cells that promote paternity? *Micron* 29, 267–280.
Buckland-Nicks, J. & Chia F-S. (1986) Fine structure of Sertoli cells in three marine snails with discussion on the functional morphology of Sertoli cells in general. *Cell and Tissue Research* 245, 305–313.
Charnov, E.L. (1996) Sperm competition and sex allocation in simultaneous hermaphrodites. *Evolution and Ecology* 10, 457–462.
Chen, S.H., Xia, L.P., Dahms, H.U., Peng, X. & Ying, X.P. (2015) The ultrastructural characteristics of spermatogenesis in *Onchidium struma* (Pulmonata: Onchidiidae) and its functional adaptation. *Italian Journal of Zoology* 82, 1–10.
Coggeshall, R.E. (1972) The muscle cells of the follicle of the ovotestis in *Aplysia* as the probable target organ for bag cell extract. Annales *Zoologic*i 12, 521–523.
Cunha, R., Rodrigues, A. & Sousa, H. (1998) The albumen gland as a maturation diagnostic organ in *Oxychilus (Drouetia) atlanticus* (Stylommatophora, Zontidae). *Iberus* 16, 75–84.
Deshpande, U.D. & Nagabhushanam, R. (1983) Annual reproductive cycle of marine pulmonate, *Onchidium verruculatum* (Cuvier) and its control by environmental factors. *Indian Journal of Marine Sciences* 12, 122–124.
De Witt, T.J. (1996) Gender contests in a simultaneous hermaphrodite snail: a size advantage model for behavior. *Animal Behavior* 51, 345–351.
Dykstra, M.J. (1993) *A Manual of Applied Techniques for Biological Electron Microscopy*. Plenum Press, New York.
Eckelbarger, K.J. & Blades-Eckelbarger, P. (1989) Structure of the ovotestis and evidence for heterosynthetic incorporation of yolk precursors in the oocytes of the nudibranch mollusk, *Spurilla neapolitana*. *Journal of Morphology* 201, 105–118.
Favard, P. & Carasso, N. (1958) Origine et ultrastructure des plaquettes vitellines de la planorbe. *Archives d'anatomie microscopique et de morphologie expérimentale* 47, 211–229.
Griffond, B. & Bolzoni-Sungur, D. (1986) Stages of oogenesis in the snail, *Helix aspersa*: cytological, cytochemical and ultrastructural studies. *Reproduction, Nutrition and Development* 26, 461–474.
Healy, J.M. (2001) Spermatogenesis and oogenesis. In: Barker, G.M. (Ed), *The Biology* of *Terrestrial Molluscs*. CABI Publishing, Wallingford, UK, pp. 357–382.
Heller, J. (1990) Longevity in molluscs. *Malacologia* 31, 259–295.
Heller, J. (2001) Life history strategies. In: Barker, G.M. (Ed.), *The Biology of Terrestrial Molluscs*. CABI Publishing, Wallingford, UK, pp. 413–445.
Hermann, P.M., Genereux, B. & Wildering, W.C. (2009) Evidence for age-dependent mating strategies in the simultaneous hermaphrodite snail, *Lymnaea stagnalis* (L.). *Journal of Experimental Biology* 212, 3164–3173.
Horn, A.C.M., Achaval, M. & Zancan, D.M. (2005) The annual reproductive cycle of the snail *Megalobulimus abbreviatus* (Bequaert, 1948) (Gastropoda, Pulmonata). *Brazilian Journal of Biology* 65, 459–467.
Jong-Brink, M. De., Boer, H.H., Hommes, T.G. & Kodde, A. (1977). Spermatogenesis and the role of Sertoli cells in the freshwater snail *Biomphalaria glabrata*. *Cell and Tissue Research* 181, 37–58.
Jong-Brink, M. De., Boer, H.H. & Joose, J. (1983) Molluska. In: Adiyodi, K.G. & Adiyodi, R.G. (Eds.), *Reproductive Biology of Invertebrates*, John Wiley, New York, pp. 297–355.
Jong-Brink, M. De., De Wit, A., Kraal, G. & Boer, H.H. (1976) A light and electron microscope study on oogenesis in the fresh water pulmonate slug *Biomphalaria glabrata*. *Cell and Tissue Research* 171, 195–219.
Jong-Brink, M. De., Schot, L.P., Schoenmakers, H.J. & Baergamin Sassen, M.J.M. (1981) A biochemical and quantitative electron microscope study on steroidogenesis in ovotestis and digestive gland of the pulmonate slug *Lymnaea stagnalis*. *General and Comparative Endocrinology* 45, 30–38.
Joosse, J. & Reitz, D. (1969) Functional anatomical aspects of the ovotestis of *Lymnaea stagnalis*. *Malacologia* 9, 101–109.
Jordaens, K., Pinceel, J. & Backeljau, T. (2005) Mate choice in the hermaphroditic land snail *Succinea putris* (Stylommatophora: Succineidae). *Animal Behaviour* 70, 329–337.
Jörger, K.M., Stöger, I., Kano, Y., Fukuda, H., Knebelsberger, T. & Schrödl, M. (2010) On the origin of Acochlidia and other enigmatic euthyneuran gastropods, with implications for the systematics of Heterobranchia. *BMC Evolutionary Biology* 10, 323.
Kimura, K., Hirano, T., Chiba, S. (2015) Assortative mating with respect to size in the simultaneously hermaphroditic land snail *Bradybaena pellucida*. *Acta Ethologica*. 18, 265–268.
Kocot, K.M., Halanych, K.M. & Krug, P.J. (2013) Phylogenomics supports Panpulmonata: opisthobranch paraphyly and key evolutionary steps in a major radiation of gastropod molluscs. *Molecular Phylogenetics and Evolution* 69, 764–771.
Kulkarni, A.B. (1973) The anatomy and histology of the reproductive system of the land slug, *Laevicaulis alte*. *Marathwada University Journal of Sciences* 12, 61–69.
Leonard, J.L. (2005) Bateman's principle and simultaneous hermaphrodites: a paradox. *Integrative and Comparative Biology* 45, 856–873.
Lofts, B. & Bern, H.A. (1972) The functional morphology of steroidogenic tissues. In: Idler, D.R. (Ed.), *Steroids in Non-Mammalian Vertebrates*. Academic Press, New York, pp. 37–125.
Luchtel, D.L. (1972a) Gonadal development and sex determination in pulmonate mollusks *Arion circumscriptus*. *Zeitschrift für Zellforschung* 130, 279–301.
Luchtel, D.L. (1972b) Gonadal development and sex determination in pulmonate mollusks. 1. *Arion ater rufus* and *Deroceras reticulatum*. *Zeitschrift für Zellforschung* 130, 302–311.
Maekawa, M., Kamimura, K. & Nagano, T. (1996) Peritubular myoid cells in the testis: Their structure and function. *Archives of Histology and Cytology* 59, 1–13.
Nagabhushanam, R. & Kulkarni, A.B. (1971) Reproductive biology of the land slug, *Laevicaulis alte*. *Rivista di Biologia* 64, 15–33.
Nakadera, Y., Swart, E.M., Maas, J.P.A., Montagne-Wajer, K., Ter Maat, A. & Koene, J.M. (2015) Effects of age, size, and mating history on sex role decision of a simultaneous hermaphrodite. *Behaviour Ecology* 26, 232–241.
Nørrevang, A. (1968) Electron microscopic morphology of oogenesis. *International Review of Cytology* 23, 113–186.
Norton, C.G. & Bronson J.M. (2006) The relationship of body size and growth to egg production in the hermaphroditic freshwater snail, *Helisoma trivolvis*. *Journal of Molluscan Studies* 72, 143–147.
Odiete, W.O. (1982) Fine structural studies on the ovotestis of *Archachatina marginata* (Swainson) (Pulmonata: Stylommatophora). *Malacologia* 22, 137–143.
O'Donavan, P. & Abraham, M. (1987) Somatic tissue-male germ cell barrier in three hermaphrodite invertebrates:

Dugesia biblica (Platyhelminthes), *Placobdella costata* (Annelida), and *Levantina hierosolyma* (Mollusca). *Journal of Morphology* 192, 217–227.

Ohbayashi-Hodoki, K., Ishihama, F. & Shimada, M. (2004) Body size–dependent gender role in a simultaneous hermaphrodite freshwater slug, *Physa acuta*. *Behavioural Ecology* 15, 976–981.

Okamura, F. & Nishiayama, H. (1976) The early development of the tail and the transformation of the shape of the nucleus of the spermatid of the domestic fowl, *Gallus gallus*. *Cell and Tissue Research* 169, 345–359.

Otsuka, C., Rouger, Y. & Tobach, E. (1980) A possible relationship between size and reproductive behavior in a population of *Aplysia punctata* (Cuvier, 1803). *Veliger* 23, 159–162.

Pal, P. & Hodgson, A.N. (2002) An ultrastructural study of oogenesis in a planktonic and a direct developing species of *Siphonaria* (Gastropoda: Pulmonata). *Journal of Molluscan Studies* 68, 337–344.

Parivar, K. (1978) A histological survey of gonadal development in *Arion ater* (Mollusca, Pulmonata). *Journal of Molluscan Studies* 44, 250–264.

Parivar, K. (1980) Differentiation of the Sertoli cells and post reproductive epithelial cells in the hermaphrodite gland of *Arion ater* (L.) (Mollusca, Pulmonata). *Journal of Molluscan Studies* 46, 139–147.

Quattrini, D. & Lanza, B. (1964) Osservazioni sulla ovogenesi e sulla spermatogenesi di *Vaginulus borellianus* (Colosi) Mollusca Gastropoda Soleolifera. *Bolletino di Zoologia* 31, 541–553.

Quatrini, D. & Lanza, B. (1965) Ricerche, Sulla biologia di *Vernocellidae* (Gastropoda-Soliolifera). II. Structuradella gonad ovogenesi e spermatogenesis in *Vaginulus borellianus* (Colosi) e in *Laevicaulis alte* (Férussac). *Monitore Zoologica Italiano* 73, 3–60.

Rakshit, S., Chaki, K.K., Sarkar, A.K. & Misra, K.K. (2005) Cytomorphology of ovotestis of a pulmonate mollusk, *Achatina fulica*. *Proceedings of the Zoological Society Calcutta* 58, 93–104.

Raut, S.K. & Panigrahi, A. (1990) Feeding rhythm in the garden slug *Laevicaulis alte* (Soleolifera: Veronicellidae). *Malacological Review* 23, 39–46.

Rigby, J.E. (1982) The fine structure of differentiating spermatozoa and Sertoli cells in the gonad of the pond snail, *Lymnaea stagnalis*. *Journal of Molluscan Studies* 48, 111–123.

Roy, S., Chaki, K.K., Nag, T.C. & Misra, K.K. (2016) Ultrastructure of ovotestis of young and adult of a pulmonate mollusk, *Macrochlamys indica* (Benson, 1832). *Journal of Microscopy and Ultrastructure* 4, 184–194.

Roy, S., Chaki, K.K., Nag, T.C. & Misra, K.K. (2018) Ultrastructure of gametogenesis in the ovotestis of an estuarine pulmonate slug, *Onchidium tigrinum* (Stoliczka 1869). *Molluscan Research* 38, 243–257.

Rustom, R., Saffrich, R., Markovic, I., Walther, P. & Gerdes, H.H. (2004) Nanotubular highways for intercellular organelle transport. *Science* 303, 1007–1010.

Sabelli, B. & Sabelli, F.S. (1980) Sexualization of germ cells in *Papollifera papillaris* (Muller). (Pulmonata, Stylommatophora). *Italian Journal of Zoology* 14, 19–26.

Selmi, M.G., Giusti, F. & Manganelli, G. (1988) The fine structure of the mature spermatozoon of *Onchidella celtica* (Cuvier) (Mollusca: Gastropoda) and its phylogenetic implications. *Journal of Ultrastructure and Molecular Structure Research* 99, 107–123.

Silva, da R.F., Cubas, J.J.M. & De Moraes J. (2009) Aspectos histológicos das gônadas hermafroditas de *Biomphalaria glabrata* e *Bradybaena similaris* (Mollusca, Gastropoda, Pulmonata). *Papéis Avulsos de Zoologia* 49, 459–466.

Skinner, M.K. & Fritz, I.B. (1985) Testicular peritubular cells secrete a protein under androgen control that modulates Sertoli cell functions. *Proceedings of the National Academy of Sciences*, USA 82, 114–118.

Staib, R. & Ribi, G. (1995) Size-assortative mating in a natural population of *Viviparus ater* (Gastropoda: Prosobranchia) in Lake Zurich, Switzerland. *Journal of Molluscan Studies* 61, 237–247.

Starke, F.J. (1971) Elektronenmikroskopische Untersuchung der Zwittergonadenacini von *Planorbarius corneus* L. (Basommatophora). *Zeitschrift Zellforsch* 119, 483–514.

Taylor, G.T. & Anderson, E. (1969) Cytochemical and fine structural analysis of oogenesis in the gastropod, *llyanassa obsoleta*. *Journal of Morphology* 129, 211–247.

Terakado, K. (1974) Origin of yolk granules and their development in the snail *Physa acuta*. *Journal of Electron Microscopy* 23: 99–106.

Till-Bottraud, I., Joly, D., Lachaise, D. & Snook, R.R. (2005) Pollen and sperm heteromorphism: convergence across kingdoms? *Journal of Evolutionary Biology* 18, 1–18.

Tokuyasu, K.T., Peacock, W.J. & Hardy, R.W. (1972) Dynamics of spermiogenesis in *Drosophila melanogaster* II. Coiling process. *Zeitschrift* für *Zellforschung* und *mikroskopische Anatomie* 127, 492–525.

Tomiyama, K. (1995) Mate choice in a simultaneously hermaphroditic land slug, *Achatina fulica* (Stylommatophora: Achatinidae). In: Guerra, A., Rolán, E. & Rocha, F. (Eds), *Proceedings of the 12th International Malacological Congress*, Vigo 12, pp. 279–280.

Tompa, A. (1984) Land snails (Stylommatophora) In: Saleuddin, A.S.M. & Wilbur, K.M. (Eds), *The Mollusca*, Academic Press, London, Vol. 7, pp. 47–140.

van der Wal, U.P. (1974) De mobilizatie van de dooier van *Lymnaea stagnalis* L. Ph. D. Thesis, University of Utrecht.

Yusa, Y. (1996) The effects of body size on mating features in a field population of the hermaphroditic sea hare *Aplysia kurodai* Baba, 1937. *Journal of Molluscan Studies* 62, 381–386.